


SIRT1 regulates macrophage self-renewal

Francesco Imperatore¹, Julien Maurizio¹, Stephanie Vargas Aguilar^{1,2}, Clara J Busch², Jérémy Favret^{1,2}, Elisabeth Kowenz-Leutz², Wilfried Cathou¹, Rebecca Gentek¹, Pierre Perrin¹, Achim Leutz², Carole Berruyer^{1,†} & Michael H Sieweke^{1,2,*†} 

Abstract

Mature differentiated macrophages can self-maintain by local proliferation in tissues and can be extensively expanded in culture under specific conditions, but the mechanisms of this phenomenon remain only partially defined. Here, we show that SIRT1, an evolutionary conserved regulator of life span, positively affects macrophage self-renewal ability *in vitro* and *in vivo*. Overexpression of SIRT1 during bone marrow-derived macrophage differentiation increased their proliferative capacity. Conversely, decrease of SIRT1 expression by shRNA inactivation, CRISPR/Cas9 mediated deletion and pharmacological inhibition restricted macrophage self-renewal in culture. Furthermore, pharmacological SIRT1 inhibition *in vivo* reduced steady state and cytokine-induced proliferation of alveolar and peritoneal macrophages. Mechanistically, SIRT1 inhibition negatively regulated G1/S transition, cell cycle progression and a network of self-renewal genes. This included inhibition of E2F1 and Myc and concomitant activation of FoxO1, SIRT1 targets mediating cell cycle progression and stress response, respectively. Our findings indicate that SIRT1 is a key regulator of macrophage self-renewal that integrates cell cycle and longevity pathways. This suggests that macrophage self-renewal might be a relevant parameter of ageing.

Keywords cell cycle regulation; macrophage; replicative life span; self-renewal; sirtuins

Subject Categories Development & Differentiation; Immunology

DOI 10.15252/embj.201695737 | Received 15 September 2016 | Revised 30 May 2017 | Accepted 2 June 2017 | Published online 12 July 2017

The EMBO Journal (2017) 36: 2353–2372

Introduction

Macrophages reside in essentially all tissues of the body and contribute to diverse functions such as tissue development, homeostasis, repair and immunity (Wynn *et al*, 2013). Under challenge conditions, during inflammation or in tissues with high turnover, they can be replaced by infiltrating monocytes originating from hematopoietic stem cells (HSCs) (Geissmann *et al*, 2010; Shi

& Pamer, 2011; Mildner *et al*, 2013; Ginhoux & Jung, 2014). More recently, it has been demonstrated that resident tissue macrophages can also be embryo-derived and self-maintain long term by local proliferation independently of HSCs (Sieweke & Allen, 2013; Gentek *et al*, 2014; Lavin *et al*, 2015; Ginhoux & Williams, 2016; Perdiguero & Geissmann, 2016; Prinz *et al*, 2017). These observations indicated that macrophages might have inherent self-renewal mechanisms that classically have been associated with stem cells (Sieweke & Allen, 2013). Indeed, we could recently show that a network of genes governing macrophage self-renewal overlaps substantially with that controlling self-renewal in embryonic stem (ES) cells (Soucie *et al*, 2016). These genes are under the control of macrophage-specific enhancers, already present in the quiescent state, but repressed by the macrophage transcription factors c-Maf and MafB. The self-renewal gene network can be activated in macrophage populations that express low levels of these Maf transcription factors either constitutively, as is the case for alveolar macrophages (AMs) or upon cytokine stimulation, as observed for example in M-CSF-induced peritoneal macrophages (Soucie *et al*, 2016). As a consequence, monocyte or bone marrow-derived macrophages with a genetic deletion of MafB and c-Maf (hereafter referred to as *Maf*-DKO macrophages) mimic this process and self-renew indefinitely in culture in the presence of macrophage colony-stimulating factor (M-CSF), without transformation or loss of their mature functional phenotype (Aziz *et al*, 2009; Soucie *et al*, 2016).

Here, we further investigated the molecular mechanisms of the extended, possibly indefinite, replicative life span of mature differentiated macrophages by focusing on sirtuin family proteins, which affect similar processes in other cell types and organisms. The founding member of this family, silent information regulator 2 (SIR2) from *Saccharomyces cerevisiae*, was found to extend the replicative life span of yeast (Sinclair & Guarente, 1997; Kaeberlein *et al*, 1999). Mammals have seven sirtuin homologues (SIRT1–7) in different subcellular compartments (Frye, 2000; North & Verdin, 2004; Guarente, 2013). The closest mammalian homologue SIRT1, residing in nucleus and cytoplasm, has been shown to play important roles in physiological processes affecting organismal longevity as well as stem cell function and self-renewal (Chung *et al*, 2010; Boutant & Canto, 2014).

¹ Aix Marseille Université, CNRS, INSERM, CIML, Marseille, France

² Max-Delbrück-Centrum für Molekulare Medizin in der Helmholtzgemeinschaft (MDC), Berlin, Germany

*Corresponding author. Tel: +33 4912 69438; E-mail: sieweke@ciml.univ-mrs.fr

[†]These authors contributed equally to this work

Although initial reports of organismal longevity prolonging effects of sirtuins in *D. melanogaster* and *C. elegans* models remain controversial, it appears that sirtuins participate in many processes that affect life span, such as inflammation, cellular senescence, apoptosis, cell cycle control and changes in energy and oxygen metabolism occurring during ageing and anti-ageing regimens such as caloric restriction (reviewed in Houtkooper *et al*, 2012; Guarente, 2013; Chang & Guarente, 2014; Pouloule & Raju, 2015).

Tissue homeostasis is dependent on somatic stem cells and age-dependent tissue degeneration is associated with successive loss of stem cell function and numbers (Liu & Rando, 2011; Oh *et al*, 2014). Remarkably in this context, SIRT1 appears to be important for the function and self-renewal capability of a variety of stem cells. SIRT1 protein and mRNA levels are elevated in mouse and human ES cells compared to differentiated tissues (Calvanese *et al*, 2010; Saunders *et al*, 2010) and are required for stem cell maintenance (Han *et al*, 2008). SIRT1 inactivation was also shown to reduce cellular proliferation and to accelerate senescence of human mesenchymal stem cells (MSCs; Yuan *et al*, 2012). Furthermore, SIRT1 deletion in HSCs was shown to cause characteristic changes normally associated with HSC ageing, such as loss of genomic stability, increased sensitivity to DNA damage, myeloid lineage skewing and premature stem cell exhaustion in serial transplantation assays (Singh *et al*, 2013; Rimmelle *et al*, 2014). Reversely, overexpression of SIRT1 increased cell proliferation and cell cycle progression in MSCs (Yuan *et al*, 2012), in spermatogonial stem cells (Niu *et al*, 2016) and in skeletal muscle stem and progenitor cells (Rathbone *et al*, 2009). Consistent with this, replenishment of the SIRT substrate nicotinamide adenine dinucleotide (NAD^+) in old mice reverted neuronal, melanocyte and muscle stem cell exhaustion in a SIRT1-dependent fashion (Zhang *et al*, 2016a). Besides other sirtuins that might also influence stem cell self-renewal, as has been reported for SIRT3 in HSCs (Brown *et al*, 2013), these observations establish SIRT1 as a key regulator for the maintenance of self-renewal capacity in stem cells.

Sirtuins are class III histones deacetylases (HDACs) that catalyse the deacetylation of acetyl-lysine residues of histone proteins in a reaction cleaving the co-factor NAD^+ (Haigis & Sinclair, 2010). In addition to histones, SIRT1 also deacetylates non-histone substrates, including p53, Myc and FoxO transcription factors (Cheng *et al*, 2003; Motta *et al*, 2004; Frescas *et al*, 2005; Kitamura *et al*, 2005; Mao *et al*, 2011) and cell cycle regulators such as retinoblastoma protein (Rb; Wong & Weber, 2007), which promotes G1-S phase transition by release of E2F transcription factors from an inhibitory complex with Rb (Sherr, 1995, 1996; Sherr & Roberts, 1999). The effect of SIRT1 on Myc and FoxO1/FoxO3 transcription factors can regulate several cellular pathways including cell cycle control and stress response (Yuan *et al*, 2009; Sharma *et al*, 2012). FoxO family proteins are involved in important cellular processes such as stress resistance, metabolism, cell cycle arrest, apoptosis and longevity (Martins *et al*, 2016).

Based on these observations and our own data that macrophages share a self-renewal gene network with stem cells (Soucie *et al*, 2016), we investigated whether SIRT1 could regulate proliferation and replicative life span in differentiated macrophages. To address this question, we studied the role of SIRT1 in alveolar macrophages that display unlimited expansion potential and in Maf-DKO macrophages in cell culture, as well as in peritoneal and alveolar

macrophages *in vivo*. We performed loss of function analysis of SIRT1 by shRNA inactivation, CRISPR/Cas9 deletion and chemical inhibition with Inauhzin, a SIRT1 antagonist (Zhang *et al*, 2012) or with the natural inhibitor nicotinamide (NAM). This amide form of vitamin B3 is generated as a by-product of NAD^+ cleavage in the sirtuin catalysed deacetylation reaction and inhibits sirtuin activity by negative feedback (Jackson *et al*, 2003; Sauve & Schramm, 2003; Avalos *et al*, 2005).

Using these diverse and complementary approaches, we demonstrate that inhibition of SIRT1 limits the self-renewal ability of terminally differentiated macrophages in culture and in different macrophage populations *in vivo*. Reversely, the overexpression of SIRT1 in bone marrow-derived macrophages improved their proliferative capacity. Furthermore, we show that the positive role of SIRT1 in macrophage self-renewal involves inhibition of FOXO1 and de-repression of E2F and Myc pathways.

Results

SIRT1 is required for macrophage self-renewal

To address the potential role of SIRT1 in regulating self-renewal in macrophages, we first assessed its expression in Maf-DKO macrophages. SIRT1 showed threefold higher protein levels in Maf-DKO cells as compared to wild-type bone marrow-derived macrophages (WT BMMs) (Fig 1A and B). Based on its reported role in stem cell self-renewal (Han *et al*, 2008; Rathbone *et al*, 2009; Yuan *et al*, 2012; Niu *et al*, 2016; Zhang *et al*, 2016a), we further proceeded to knockdown SIRT1 by means of specific short hairpin RNA (shRNA) to evaluate the functional importance of SIRT1 for Maf-DKO macrophage self-renewal. Two retroviral shRNA constructs against SIRT1 were able to specifically induce a twofold to fourfold down-regulation of target transcripts (Fig 1C). To test the effect of this down-regulation on macrophage self-renewal, we infected Maf-DKO macrophages and analysed colony-forming ability in M-CSF containing semi-solid medium. SIRT1 shRNA-infected Maf-DKO macrophages showed a strong reduction in the colony-forming ability that correlated with the reduction in sirtuin expression levels (Fig 1D and E). We further focused on anti SIRT1 shRNA-construct #2, which showed the strongest phenotype in terms of colony size and number (Fig 1D and E) as well as reduction in mRNA (Fig 1C) and protein expression (Fig 1F and G). Using this construct we further analysed the role of SIRT1 in cell cycle regulation. DNA content analysis by propidium iodide staining revealed a reduction of the fraction of cycling cells in SIRT1-knockdown macrophages from 34% to 23% in S/G2 and an increase from 64 to 75% of cells in G1 phase (Fig 1H and I). We also used CRISPR/Cas9-mediated deletion of SIRT1 to analyse the impact on alveolar macrophages, a macrophage population that naturally expresses low Maf levels and exhibits self-renewal capacity (Soucie *et al*, 2016). When we infected Cas9-expressing AMs with SIRT1-specific CRISPR gRNA vectors, we observed 30% less colonies in SIRT1 deleted AMs compared to controls (Fig 1J). Since tide analysis (Appendix Fig S1), revealed SIRT1 deletion in 60% of the cells, this indicated a ~50% reduction in colony formation in SIRT1-deficient cells. Finally, we performed gain of function experiments by infecting bone marrow-derived macrophages from mice with constitutive expression of reverse tet

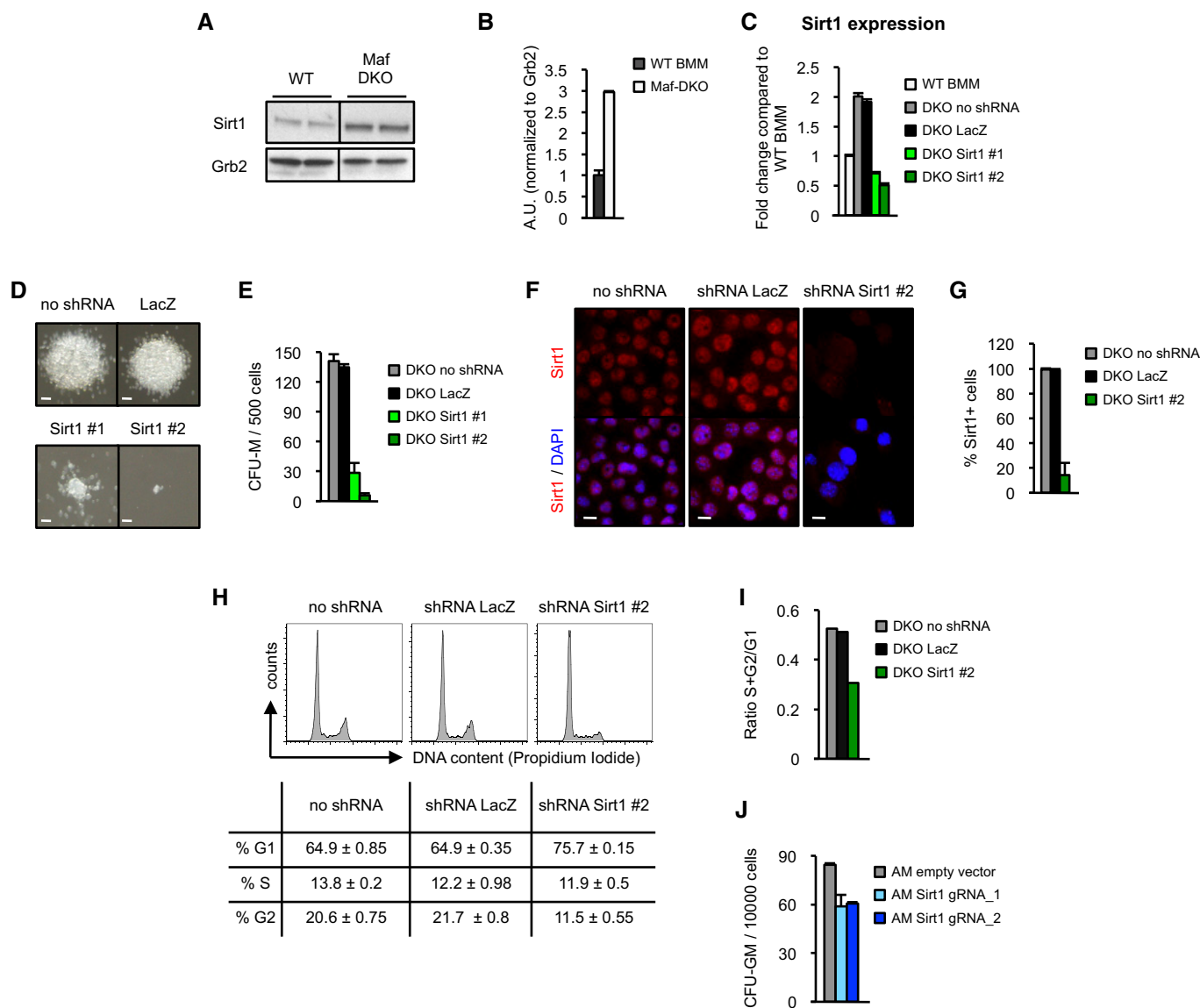


Figure 1. SIRT1 inactivation inhibits macrophage self-renewal.

A Immunoblot for SIRT1 protein comparing bone marrow-derived wild-type (WT BMM) and MafB/c-Maf double knockout (Maf-DKO) macrophages. Grb2 antibody was used as loading control.

B Quantification of panel (A). Shown are Sirt1/Grb2 ratios (arbitrary units, A.U.), normalized to Grb2. Error bars indicate the standard error of the mean. Each condition was done in duplicate; data represent the pool of two independent experiments.

C Quantitative PCR for the expression of SIRT1 comparing Maf-DKO macrophages infected with indicated shRNA vectors to non-infected Maf-DKO and wild-type (WT) macrophages. Shown are fold changes of the average values normalized to HPRT of two independent experiments and standard error of the mean.

D Effect of SIRT1 inactivation on the colony formation potential of Maf-DKO macrophages. Phase contrast magnification $\times 10$. Each condition was done in duplicate; the results shown are representative of two independent experiments. Scale bars = 50 μ m.

E Quantification of panel (D). Data represent the pool of two independent experiments. Error bars indicate SEM.

F Immunostaining for SIRT1 (red) on Maf-DKO macrophages infected with shRNA vectors against LacZ or SIRT1. DAPI (blue) was used to stain DNA. Each condition was done in duplicate; the results shown are representative of two independent experiments. Scale bars = 20 μ m.

G Quantification of panel (F). Error bars indicate SEM.

H DNA content analysis of Maf-DKO macrophages infected with shRNA vectors against SIRT1 or LacZ. Each condition was done in duplicate; the results shown are representative of two independent experiments. Table indicates the percentage of cells in indicated cell cycle phases.

I Quantification of panel (H), represented as ratio between proliferating (S+G2) and resting cells (G1). Data represents the pool of two independent experiments.

J Analysis of colony formation potential after SIRT1 deletion by CRISPR gRNA vector infection of Cas9 expressing alveolar macrophages. Each condition was done in duplicate. Deletion efficiency of Sirt gRNA_1 and sirt gRNA_2 was evaluated by TIDE analysis (Appendix Fig S1) and corresponds to 60.9 and 44.7%, respectively. Error bars indicate SEM.

Source data are available online for this figure.

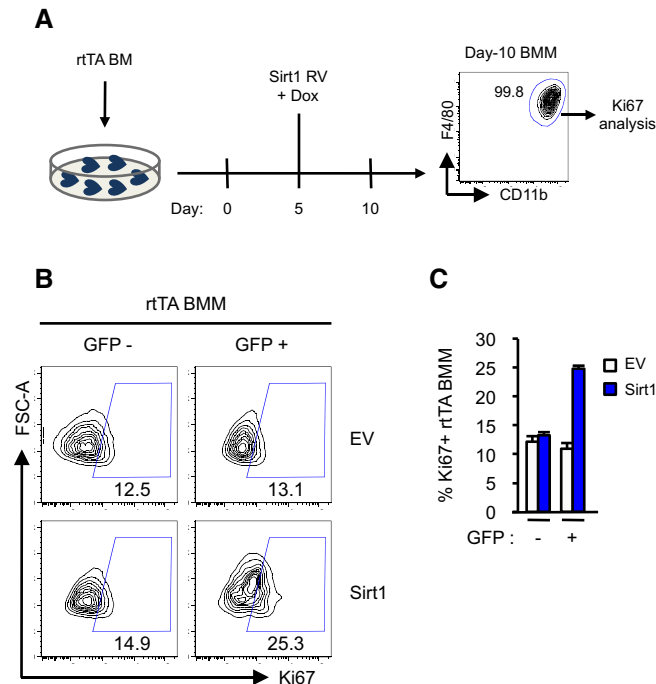


Figure 2. SIRT1 overexpression increases macrophage proliferation.

- A** Experimental scheme of rTA BMM differentiation and infection with tetO SIRT1 retrovirus. FACS shows purity of macrophage population as 99.8% F4/80⁺/CD11b⁺ cells.
- B** Intracellular FACS staining of Ki67 on rTA bone marrow-derived macrophages (CD11⁺ F4/80⁺) infected with retrovirus expressing doxycycline-inducible SIRT1 and constitutive GFP or empty vector (EV), 5 days post-infection.
- C** Quantification of panel (B). The results shown are representative of two independent experiments. Error bars indicate the standard error of the mean.

transactivator (rtTA) with vectors containing a GFP reporter and a *sirt1* gene under the control of a tet responsive element (TRE). This allows doxycycline-inducible SIRT1 expression and constitutive GFP expression during macrophage differentiation (Fig 2A). Using Ki67 staining, we observed a significant enhancement of proliferative capacity in SIRT1-expressing macrophages compared to empty vector or uninfected control cells 5 days after infection and doxycycline induction (Fig 2B and C). Taken together, these data show that SIRT1 is a critical mediator of self-renewal capacity in differentiated macrophages.

Pharmacological SIRT1 inhibition abrogates macrophage self-renewal capability

We next tested whether pharmacological inhibition with NAM, a natural sirtuin inhibitor, also resulted in the functional impairment of macrophage self-renewal. NAM is generated as a by-product of sirtuin deacetylase activity and blocks further catalysis in a negative feedback loop (Bitterman *et al*, 2002; Avalos *et al*, 2005). As shown in Fig 3A and B, NAM inhibited the colony formation ability of Maf-DKO cells in a strictly dose-dependent manner, as revealed by reduced colony size and numbers, with the highest concentration of NAM (10 mM) completely neutralizing colony formation in M-CSF.

We also found that NAM-treated Maf-DKO macrophages showed 16-fold reduction of 5-bromo-2'-deoxyuridine (BrdU) incorporation (Fig 3C and D), demonstrating impairment of DNA synthesis compared to non-treated cells. Consistent with this, NAM also resulted in a threefold decrease in the number of cells expressing the nuclear Ki67 antigen, a marker of cycling cells (Fig 3E and F). Finally, analysis of DNA content by propidium iodide staining revealed that NAM treatment reduced the fraction of macrophages in G2/S phase from 28 to 6% and increased the percentage in G0/G1 from 71 to 94% (Fig 3G–I). Together the inhibition of macrophage self-renewal and S phase transition by NAM were similar to the effects observed for SIRT1 inactivation (Fig 1) and were thus consistent with the ability of NAM to inhibit sirtuin deacetylase activity.

However, NAM is not only a sirtuin inhibitor but also the amide form of vitamin B3 and a metabolic precursor of NAD⁺, a co-factor of the sirtuin deacetylase activity. We therefore wanted to confirm that the observed NAM effect was mediated by sirtuin inhibition and not by effects on NAD⁺ pools. To address this point, we directly compared NAM and the NAD⁺ precursor nicotinamide mononucleotide (NMN) on cell cycle progression. In contrast to NAM, NMN did not show any inhibitory effect on cell cycle progression (Fig 3J). This result was consistent with previous observations showing that NAD⁺ depletion using the drug FK866 also had no effect on Maf-DKO macrophage proliferation (Venter *et al*, 2014). NAD⁺ is also a co-factor of poly(ADP-ribose)polymerases (PARPs), enzymes that regulate DNA damage sensing, apoptosis, cellular stress and ageing, (Saldeen *et al*, 2003) and similarly release NAM as a by-product of the enzymatic reaction. In addition to its inhibitory role on sirtuins, NAM also acts as a potent inhibitor of these enzymes via a negative feedback loop. However, we did not observe any effect on macrophage self-renewal with Olaparib (Fig 3J), a specific inhibitor of PARP with no inhibitory activity on SIRT1, 2, 3 and 6 (Ekblad & Schuler, 2016).

Since NAM can inhibit several sirtuin family members, we also tested Inauhzin, a specific SIRT1 antagonist (Zhang *et al*, 2012). With this inhibitor, we also observed a similar decrease in colony-forming activity as with NAM, suggesting that NAM principally acts by SIRT1 inhibition (Fig 3J).

Finally, we verified that NAM affected SIRT1 enzymatic activity by evaluating the lysine 9 acetylation status of histone 3, a well-known target of SIRT1 deacetylase activity (Imai *et al*, 2000). Specifically, it has been demonstrated that 10 mM NAM had the same effect on inducible gene expression of WT fibroblasts as genetic SIRT1 inactivation, whereas no additional effect was seen with NAM on SIRT-deficient cells (Nakahata *et al*, 2008). In Western blot analysis, we observed a similar increase of H3K9 acetylation in Maf-DKO macrophages that were treated with NAM for the same time and concentration (Fig 3K). Together with our results on genetic inactivation of SIRT1 (Fig 1), these results indicated that NAM impairs macrophage self-renewal principally by inhibition of SIRT1 activity.

Reversible inhibition of cell cycle arrest in self-renewing macrophages

We further investigated whether the inhibition of macrophage self-renewal by NAM involved an irreversible process, such as apoptosis. However, NAM addition to Maf-DKO macrophages did not

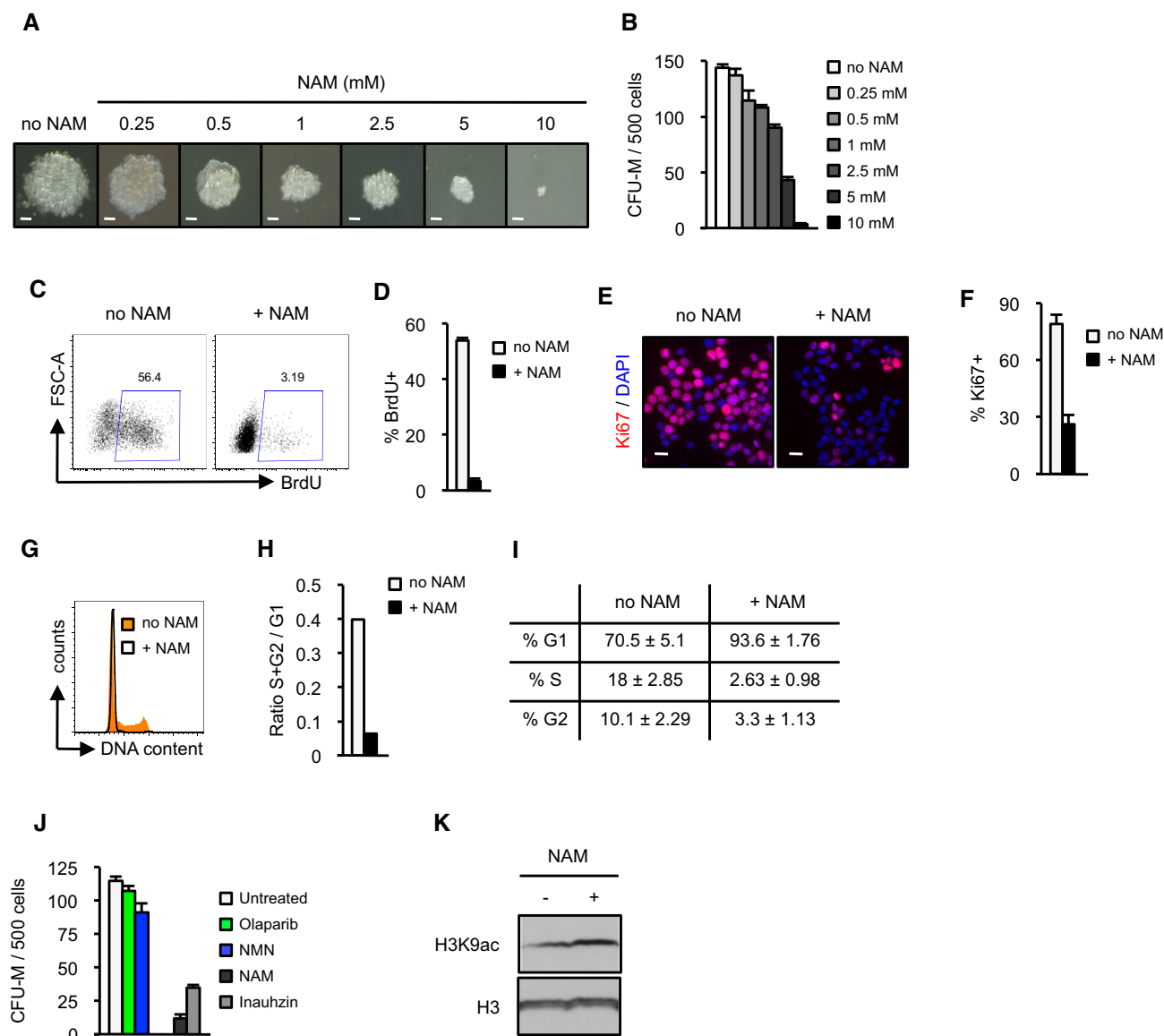


Figure 3. Pharmacological inhibition of macrophage self-renewal and cell cycle progression.

A Effect of NAM on the M-CSF-dependent colony formation ability of Maf-DKO macrophages. Phase contrast magnification $\times 10$. Each condition was done in duplicate; the results shown are representative of five independent experiments. NAM was added at day 0 and colonies were counted at day 14. Scale bars = 50 μ m.

B Quantification of panel (A). Data represent the pool of five independent experiments.

C BrdU incorporation analysis on Maf-DKO macrophages treated or not with 10 mM NAM for 48 h. Each condition was done in duplicate; the results shown are representative of two independent experiments.

D Quantification of panel (C). Data represent the pool of two independent experiments.

E Immunostaining for Ki67 antigen (red) on Maf-DKO macrophages treated or not with 10 mM NAM for 48 h. DAPI was used to stain DNA. Each condition was done in duplicate; the results shown are representative of two independent experiments. Scale bars = 20 μ m.

F Quantification of panel (E). At least 3,000 cells were counted per condition.

G DNA content analysis of Maf-DKO macrophages treated or not with 10 mM NAM for 48 h. Each condition was done in duplicate; the results shown are representative of two independent experiments.

H Quantification of panel (G), represented as ratio between proliferating (S+G2) and resting cells (G1). Data represent the pool of two independent experiments.

I Table indicates the percentage of cells in indicated cell cycle phases shown in panel (G). Error ranges indicate SEM.

J Effect of different compounds NAM, the NAD⁺ precursor nicotinamide mononucleotide (NMN), Olaparib, a PARP inhibitor, and Inauhzin, a SIRT1-specific antagonist on colony formation ability of Maf-DKO macrophages. Each condition was done in duplicate; the results shown are representative of two independent experiments.

K Enhanced histone H3 (Lys9) acetylation after SIRT1 inhibition with NAM. Total cell extracts were prepared from untreated or SIRT1 inhibitor (10 mM NAM, 20 h) treated Maf-DKO macrophages. Protein blots were incubated with anti-histone H3 (H3) or anti-histone H3 K9acetyl (H3K9ac), as indicated. Detection of histone H3 served as controls.

Data information: Error bars indicate the standard error of the mean.

Source data are available online for this figure.

result in increased apoptosis, as judged by the absence of detectable levels of activated Caspase-3, a classical marker of apoptosis that was easily observed in apoptotic beta islets used as a positive control (Fig 4A and B). To further investigate whether the cell cycle arrest observed upon NAM treatment was a reversible process, we treated Maf-DKO macrophages with NAM, then washed out NAM and continued the culture in NAM-free medium prior to cell cycle analysis. As observed before, NAM addition reduced the fraction of cycling cells (Fig 4C–E), but depletion of NAM from the culture medium induced cycle re-entry of NAM pre-treated cells (Fig 4C–E). The transitory nature of the NAM inhibitory effect was further confirmed by the re-acquisition of colony-forming ability of Maf-DKO cells upon NAM depletion (Fig 4F and G). Together these data show

that NAM treatment only transiently blocked differentiated macrophages in a reversible non-proliferative state and that self-renewal could be re-activated by NAM withdrawal.

NAM abrogates macrophage proliferation *in vivo*

We further investigated whether NAM-mediated SIRT1 inhibition also affected endogenous tissue resident macrophage self-renewal *in vivo*. We first investigated the effect of NAM inhibition on steady state proliferation of peritoneal macrophages. The peritoneal cavity contains several macrophage subsets that can be distinguished based on F4/80, CD64, TIM4 and Ly6C staining (Appendix Fig S2A; Bain *et al*, 2016). Ly6C[−], F4/80^{hi}, CD64⁺,

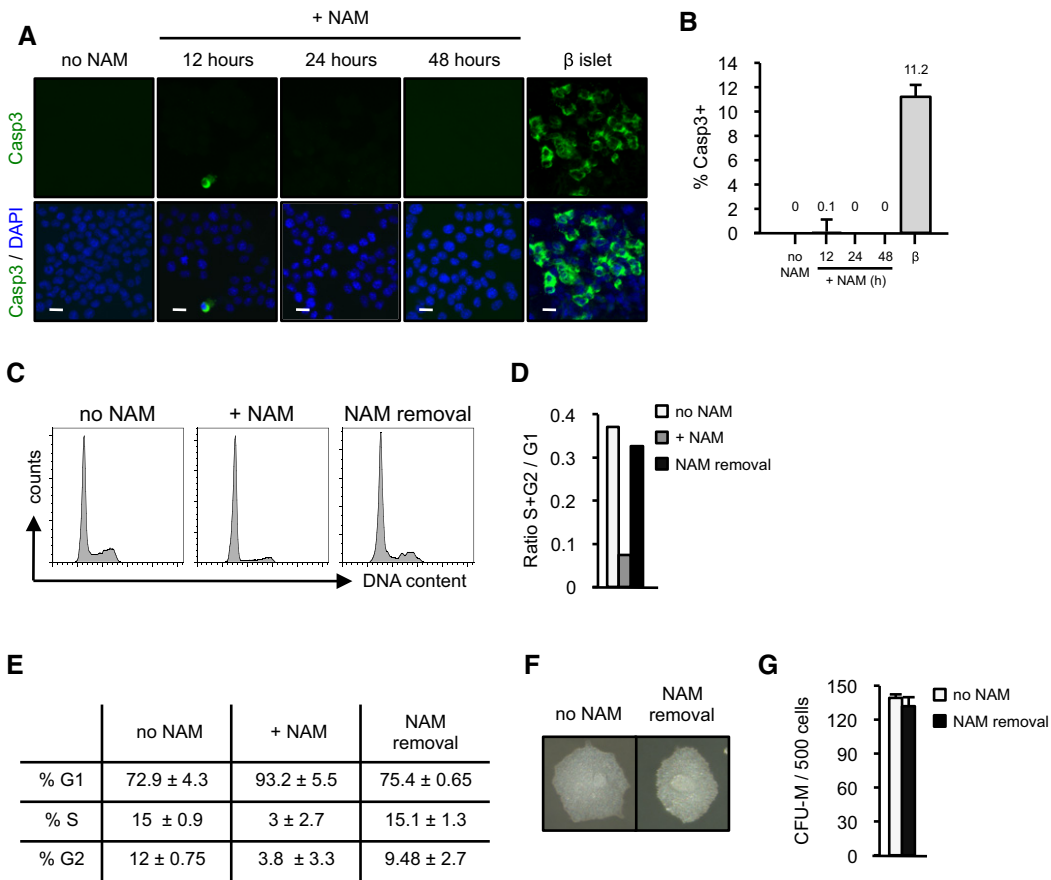


Figure 4. Reversibility of the NAM inhibition of macrophage self-renewal.

A Immunostaining for activated Caspase-3 (green) on Maf-DKO macrophages treated with NAM for 12, 24 or 48 h. Apoptotic beta islets (β) from streptozotocin-treated mice were used as positive control. DAPI was used to stain DNA. Each condition was done in duplicate; the results shown are representative of two independent experiments. Scale bars = 20 μ m.

B Quantification of panel (A). At least 3,000 cells were counted per condition.

C DNA content analysis of Maf-DKO cells pre-treated with 10 mM NAM (during 48 h) and restimulated with NAM-free medium. Each condition was done in duplicate; the results shown are representative of three independent experiments.

D Quantification of panel (C) represented as ratio between proliferating (S+G2) and resting cells (G1). Data represent the pool of three independent experiments.

E Percentage of cells in indicated cell cycle phases of samples shown in panel (D). Error ranges indicate SEM.

F Effect of NAM pre-treatment (48 h) and removal on colony formation ability of Maf-DKO macrophages. Phase contrast magnification $\times 10$. Each condition was done in duplicate; the results shown are representative of three independent experiments.

G Quantification of panel (F). Data represent the pool of three independent experiments.

Data information: Error bars indicate the standard error of the mean.

Tim4⁺ and Ly6C⁺, F4/80^{hi}, CD64⁺, Tim4⁺ represent resident peritoneal macrophage populations that in the absence of challenge contain cells of embryonic origin that may autonomously self-renew for at least several months (Bain *et al*, 2016). F4/80^{lo/-}, CD64⁺ and Ly6C⁺ represent monocyte-derived macrophages. Using Ki67 staining as a marker of cycling cells, we observed that the low rate of steady state proliferation of ~5–7% was reduced by about threefold after intra-peritoneal NAM injection in both resident peritoneal macrophage populations, whereas monocyte-derived macrophages showed no significant change (Fig 5A and B, and Appendix Fig S2B). During infection or inflammation peritoneal macrophages may significantly increase the proliferative rates over the steady state (Davies *et al*, 2011). This can be mimicked by intra-peritoneal M-CSF injection that induces increased proliferation of peritoneal macrophages (Davies *et al*, 2013; Jenkins *et al*, 2013; Gow *et al*, 2014; Soucie *et al*, 2016) by down-regulation of Maf transcription factors and activation of a self-renewal gene network (Soucie *et al*, 2016). We assessed the effect of NAM on this induced proliferative response (Fig 5C and D) by EdU incorporation as a measure for DNA synthesis and observed that in the presence of NAM the M-CSF-induced proliferation increase was abolished and reduced to background levels. Finally, we have analysed the effect of NAM on alveolar macrophages (gating strategy in Appendix Fig S3), a population of resident macrophages that is dependent on GM-CSF for autonomous self-renewal *in vivo* (Guilliams *et al*, 2013; Hashimoto *et al*, 2013). We also observed a significant twofold reduction of steady state proliferation in this macrophage population in response to NAM (Fig 5E and F).

Together our results thus demonstrated that NAM abrogated both steady state and induced proliferation of different resident M-CSF- and GM-CSF-dependent macrophage populations, suggesting that SIRT1 is of general importance for macrophage proliferation *in vivo*.

SIRT1 inhibition affects regulators of macrophage cell cycle progression

In order to identify the molecular pathways affected by SIRT1 in self-renewing Maf-DKO macrophages, we further investigated the global changes in gene expression occurring 1 and 10 h after NAM-induced SIRT1 inhibition (Fig 6A). Besides general signalling and immune function pathways, an enrichment map (Merico *et al*, 2010) based on GSEA analysis of gene sets derived from the biological process ontology group (BP:GO Biological process; <http://software.broadinstitute.org/gsea/msigdb/collections.jsp#C5>) also revealed a down-regulation of genes that are positively regulated in cellular proliferation (Fig EV1). In order to characterize in more detail which regulatory pathways of cellular proliferation might be specifically affected by SIRT1 inhibition, we used the BubbleGUM strategy of gene set enrichment analysis (GSEA; Spinelli *et al*, 2015) to visualize multiple gene sets from the open source and curated Reactome database of reactions, pathways and biological processes (Haw *et al*, 2011; Fig 6A). Consistent with the biological data and the gene ontology gene set analysis, this also identified down-regulation of cell cycle regulators and checkpoints 10 h after NAM addition (Fig 6B). More detailed comparison to gene sets affecting distinct cell cycle phases revealed that NAM caused depletion in particular gene sets of S phase and G1 to S as well as M to G1

transitions (Fig 6C). Consistent with this, analysis of individual cell cycle regulatory genes derived from the descriptive gene ontology term “Cyclins” revealed that 10 h after NAM addition central positive regulators of cycle progression during G1 phase, such as Cdk4, cyclin D1 (CcnD1) and in M phase, like cyclin B1 (CcnB1) were down-regulated and critical cell cycle inhibitors like p27/CDKN1B, Rb1, RbL1 and RbL2 were up-regulated (Fig 6D). In particular, Rb is a critical master regulator of the G₁/S transition of the cell cycle through its inhibition of E2F transcription factors (Harbour & Dean, 2000) that control gene targets important for cell cycle progression (Stevens & La Thangue, 2003). Supporting the fact that the activity of E2F factors is not regulated by changes in expression levels but by phosphorylation in late G₁ phase of the cell cycle (Fagan *et al*, 1994), NAM treatment of Maf-DKO macrophages did not result in any changes in mRNA expression of E2F factors or its DP dimerization partners (Appendix Fig S4). By contrast, immunofluorescence revealed that NAM-mediated sirtuin inhibition did not change in E2F1 protein expression levels but strongly reduced levels of its phosphorylated transcriptionally active form (Fig 6E and F). Again, we confirmed that this effect appeared to be mediated mainly by SIRT1, since its shRNA inactivation resulted in nearly identical results to NAM inhibition. This is consistent with the ability of SIRT1 to deacetylate RB and inhibit its ability to sequester the transcription factor E2F1 into an inactive form (Wong & Weber, 2007). The functional importance of this was further indicated by the observation that SIRT1 inhibition resulted in down-regulation of the E2F target gene set in the hallmark collection (<http://software.broadinstitute.org/gsea/msigdb/collections.jsp#H>) (Fig 6G). Together these observations demonstrated that the requirement of sirtuin activity for cell cycle progression involved a direct effect of SIRT1 on key regulators of cycle progression that lead to activation of E2F and its downstream targets.

SIRT1 inhibition perturbs macrophage self-renewal pathways

We further investigated whether the effect of SIRT1 on cell cycle progression was associated with mechanisms that control long-term replicative life span. Towards this end, we focused on a network of self-renewal genes shared by self-renewing macrophages and ES cells that we recently identified (Soucie *et al*, 2016). Indeed, SIRT1 inhibition with NAM resulted in the down-regulation of ES cell signature gene sets (Fig 7A) that we had found to be enriched in self-renewing macrophages (Soucie *et al*, 2016), suggesting that shared self-renewal mechanism might be affected. Indeed, we identified two significantly modulated clusters of self-renewal genes: one “early” gene set down-regulated 1 h after NAM treatment (Klf2, Klf4, Nfya, Cited2, Myc) and a second “late” group of genes (Nfyb, Eed, Cebpz, Ube2f, Cih1a, Rhoj, Akt1) down-regulated 10 h after NAM treatment (Fig 7B). These observations thus revealed the majority of previously identified self-renewal genes (12/16) to be down-regulated by NAM, including the two genes, Myc and Klf2, that form the central nodes of a cross-regulatory network of these genes (Soucie *et al*, 2016; Fig 7B and C). Since no Klf2 pathway genes were annotated in the public Molecular Signatures Database (MSigDB, <http://www.broadinstitute.org/gsea/msigdb/index.jsp>), we focused on Myc-regulated genes to further analyse the downstream targets of these central factors. In line with the reduction of Myc expression, SIRT1 inhibition by NAM also resulted in the

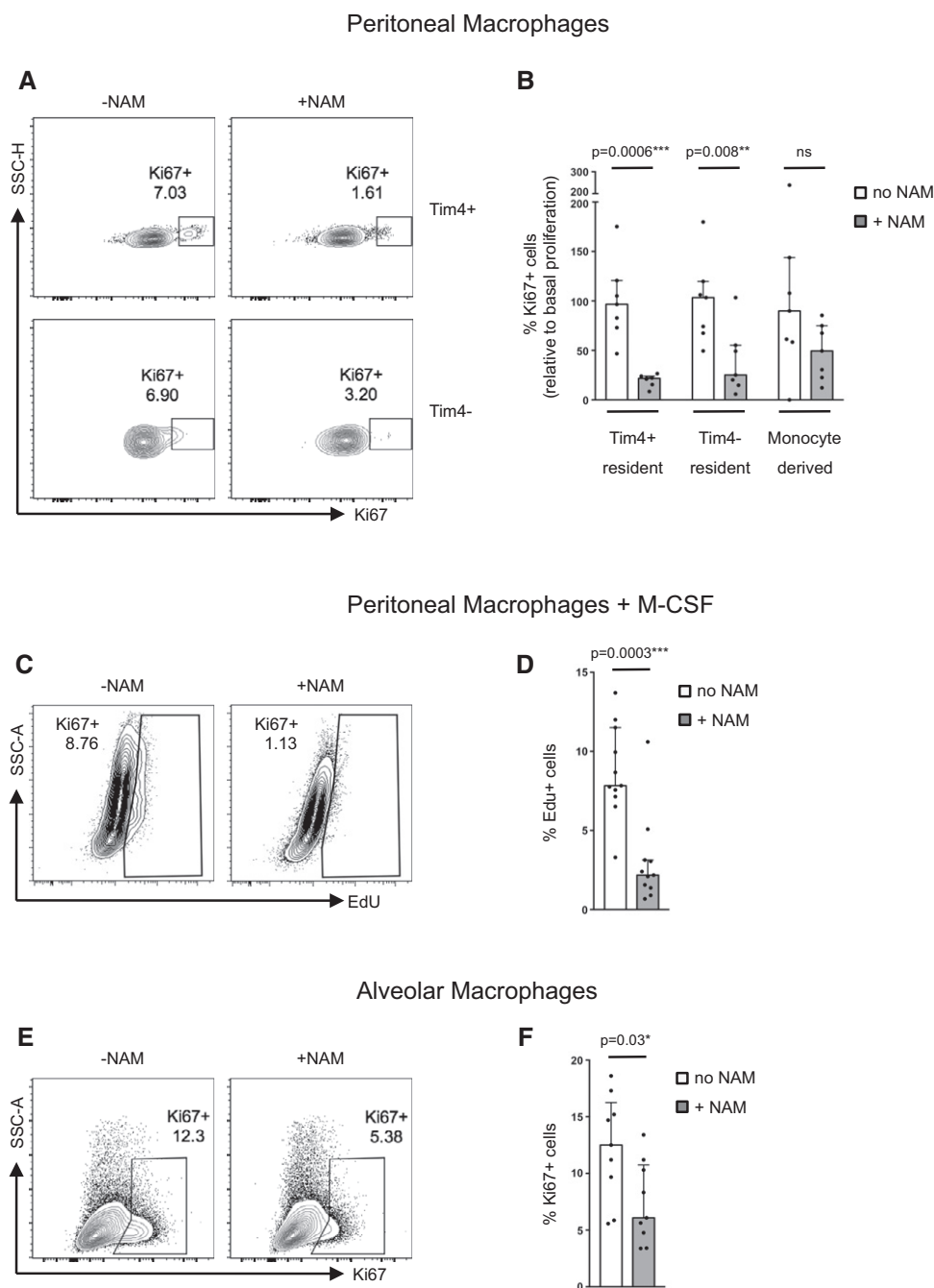


Figure 5. SIRT1 inhibition by NAM reduces macrophage proliferation *in vivo*.

- A Intracellular FACS staining of Ki67 on peritoneal macrophages from mice 48 h after I.P. NAM (10 mM) or control injections showing TIM4⁺ and TIM4⁻ resident macrophages.
- B Here is the representation of two-pooled experiments. Quantification of indicated cycling peritoneal macrophage populations expressed as a fraction of Ki67⁺ cells in control mice (100%). Data were pooled from two independent experiments. Percentage of Ki67⁺ in the respective macrophage populations are shown in Appendix Fig S2.
- C EdU incorporation analysis of M-CSF stimulated MHCII⁺ CD11b⁺ F4/80⁺ peritoneal macrophages 48 h after NAM or control i.p. injections. Representative samples for each condition are shown (*n* = 2).
- D Quantification of panel (C). Data shown are pooled from two independent experiments using 4–6 mice per group and experiment.
- E Intracellular FACS staining of Ki67 of alveolar macrophages from mice 48 h after 20 mM NAM or control i.p. injections. Representative samples for each condition are shown (*n* = 2).
- F Quantification of percentage of Ki67⁺ cells of alveolar macrophages shown in panel (E).

Data information: Statistical significance was tested using a two-tailed, unpaired, nonparametric Mann–Whitney test. Error bars correspond to the interquartile range (median values). Symbols represent individual mice.

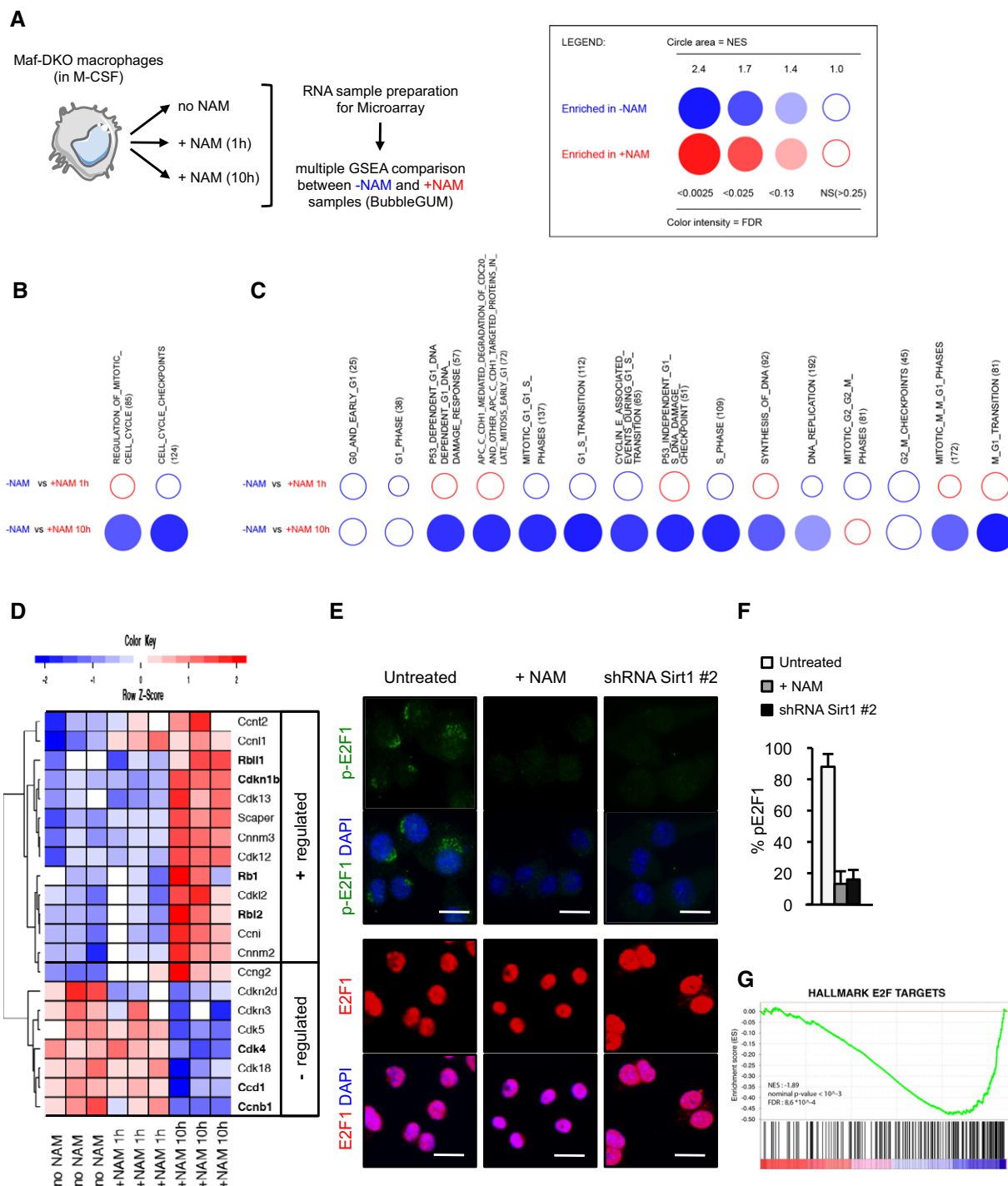


Figure 6. SIRT1 activity controls regulators of macrophage cell cycle progression.

- A Experimental scheme of microarray Maf-DKO macrophage sample generation and legend for BubbleGum analysis.
- B BubbleGUM analysis on microarray samples (Maf-DKO macrophages treated or not with NAM for 1 or 10 h) using REACTOME mitosis gene sets.
- C BubbleGUM analysis on microarray samples (Maf-DKO macrophages treated or not with NAM for 1 or 10 h) using REACTOME cell cycle phase gene sets.
- D Heat-map showing the scaled expression levels (z-score) of cyclin and cell cycle regulator related genes that were identified as coherently down-regulated (blue) or up-regulated (red) upon the administration of NAM (10 h).
- E Immunostaining for transcriptionally active phosphorylated E2F1 (p-E2F, green) and inactive non-phosphorylated E2F (E2F, red). 10 mM NAM was added for 48 h. DAPI was used for DNA staining. Scale bar, 20 μ m. The results shown are representative of three independent experiments.
- F Quantification of p-E2F1 positive cells shown as percentage of total DAPI positive cells (panel E, top). Data shown are pooled from three independent experiments. Error bars indicate SEM.
- G GSEA analysis of untreated versus 10-h NAM-treated Maf-DKO macrophages with HALLMARK E2F transcription factor target gene set.

down-regulation of Myc-activated genes annotated in hallmark, canonical pathway and genetic perturbation genes sets (Figs 7D and EV2). Collectively, transcriptomic analysis indicated that in macrophages with long-term replicative life span SIRT1 activity is required to maintain the expression of a self-renewal gene network and its downstream target genes.

Reciprocal regulation of E2F1, Myc and FoxOs activities in SIRT1 inhibited Maf-DKO macrophages

Based on our results showing the inhibition of Myc and E2F pathways by SIRT1 inhibition with NAM, we more specifically analysed annotated gene sets containing consensus-binding sites for these transcription factors in the promoter regions within ± 2 kb of the transcriptional start site (TSS; C3 TFT collection gene sets; <http://software.broadinstitute.org/gsea/msigdb/genesets.jsp?collection=TFT#>). Consistent with our previous results, upon NAM addition we observed depletion of gene sets with E2F and E-box elements recognized by Myc, Myc/Max or the related USF transcription factors (Figs 8A and EV2). Among the other transcription factors, target gene sets affected by sirtuin inhibition, those containing FoxO binding sites, were prominently represented and enriched rather than depleted (Figs 8A and EV3). When analysing significant changes in expression levels of these genes, we observed that most E2F and Myc target genes were down-regulated upon sirtuin inhibition, whereas the majority of FoxO target genes were up-regulated (Fig 8B), in line with the observation that FoxO transcription factors have been shown to induce cell cycle arrest (Schmidt *et al*, 2002; Hill *et al*, 2014).

The transcriptional activity of FoxO factors is regulated by post-translational modifications that regulate shuttling between the cytoplasm and the nucleus, binding ability and the expression of target genes (Barthel *et al*, 2005; Vogt *et al*, 2005; Hoekman *et al*, 2006). Indeed, the transcriptional activation of FoxO target genes correlated with cytoplasmic-nuclear shuttling upon SIRT1 inhibition (Fig 9A–C). Immunofluorescence analysis revealed that in cycling Maf-DKO macrophages, transcriptionally inactive FoxO1 was localized in the cytoplasm, whereas SIRT1 inhibition induced FoxO1 nuclear translocation in over 95% NAM-treated cells (Fig 9A–C). Comparable results were obtained for FoxO3 that also showed enhanced nuclear shuttling upon NAM-mediated SIRT1 inhibition (Fig EV3B–D). The knockdown of SIRT1 by shRNA induced comparable regulatory effects on cytoplasmic/nuclear shuttling of FoxO1 (Fig 9A–C). Finally, this observation was also confirmed biochemically, showing a significant increase of FOXO1 proteins in nuclear extracts after NAM treatment (Fig 9D).

Both FoxO and Myc transcription factors have also previously been shown to regulate apoptosis (Hoffman & Liebermann, 2008; Zhang *et al*, 2011), but consistent with the results shown in Fig 4A and B, no significant enrichment for apoptotic program gene sets could be detected (Appendix Fig S5A). We also did not detect any significant regulation of p53 target genes, another transcription factor that can be regulated by sirtuins and controls cell cycle, DNA repair and apoptosis pathways (Appendix Fig S5B).

Together these data indicated that NAM-dependent SIRT1 inhibition reciprocally blocks positive transcriptional regulators of cell cycle progression and self-renewal, while activating inducers of cell cycle arrest.

Discussion

In the present study, we revealed a previously unknown function of SIRT1 in the regulation of macrophage self-renewal. We have shown that SIRT1, the mammalian sirtuin homologue of the yeast Sir2 protein, is required for the self-renewal ability and M-CSF- and GM-CSF-dependent cell cycle progression of differentiated macrophages in culture and *in vivo*. We have characterized the phenomenon in three prototypic macrophage populations, alveolar macrophages, peritoneal macrophages and bone marrow-derived macrophages. Inactivation of SIRT1 revealed its essential role in macrophage self-renewal, which involved positive regulation of E2F- and Myc-dependent transcriptional pathways, while keeping FoxO transcription factors in a cytoplasmic and transcriptionally inactive state. Furthermore, we observed that macrophage cell cycle progression could be transiently inhibited by NAM, a component of vitamin B3 and natural inhibitor of SIRT1 deacetylase activity, which might be relevant to the integration of metabolism and the regulation of macrophage proliferation *in vivo*. In addition, our demonstration that a known regulator of organismal longevity is required for macrophage self-renewal capacity suggests a potential link between macrophage replicative life span and ageing.

Mechanistically, we have shown that the requirement of SIRT1 for macrophage proliferation depends on effects on cell cycle controlling pathways and previously identified self-renewal mechanisms. We recently discovered that self-renewing macrophages and ES cells share a network of self-renewal genes (Soucie *et al*, 2016). These genes are under the control of macrophage-specific enhancers that are also present in the quiescent state, but are repressed by c-Maf and MafB transcription factors. Macrophage self-renewal therefore depends on low levels of MafB and c-Maf transcription factors that can occur constitutively in alveolar macrophages or can be induced transiently by cytokines in other tissue macrophage populations (Soucie *et al*, 2016). Genetically engineered MafB/c-Maf double-deficient (Maf-DKO) macrophages permanently mimic this state and, similar to AMs, can be expanded indefinitely in culture (Aziz *et al*, 2009; Soucie *et al*, 2016). In this study, we found increased expression levels of SIRT1 in self-renewing Maf-DKO macrophages compared to quiescent wild-type bone marrow macrophages. Both inactivation with shRNA and CRISPR/Cas9 or pharmacological inhibition with different SIRT1 antagonists revealed that SIRT1 is required for macrophage self-renewal capacity. Reversely, overexpression of SIRT1 increased the low proliferative capacities of bone marrow-derived macrophages. Interestingly, SIRT1 has also been shown to positively affect the self-renewal capacity of several different types of stem cells (Rathbone *et al*, 2009; Yuan *et al*, 2012; Niu *et al*, 2016; Zhang *et al*, 2016b), including ES and iPS cells (Calvanese *et al*, 2010; Saunders *et al*, 2010). These data suggest that high levels of SIRT1 are important for active self-renewal potential in macrophages and stem cells. Consistent with this, our data demonstrate that SIRT1 inhibition in macrophages results in the reduced expression of ES cell enriched gene sets and specifically the down-regulation of the majority of self-renewal genes shared between macrophages and ES cells (Soucie *et al*, 2016), including the central key factors Myc and KLF2 and downstream targets of Myc. This indicates that SIRT1 holds important control in the regulation of the self-renewal gene network shared between macrophage and ES cells.

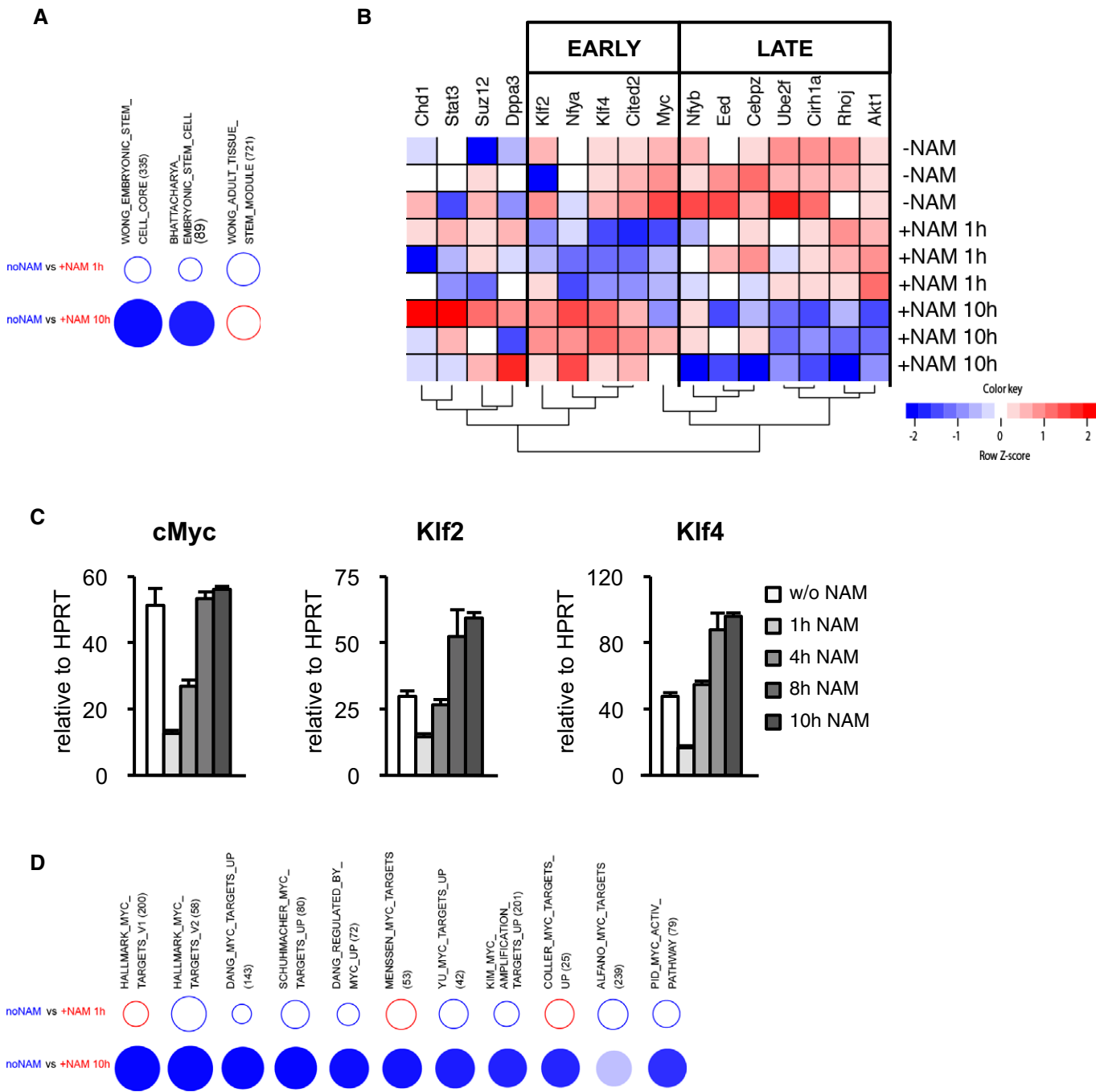


Figure 7. NAM-mediated SIRT1 inhibition perturbs macrophage self-renewal pathways.

A BubbleGUM analysis on microarray samples of Maf-DKO macrophages treated or not with NAM for 1 h or 10 h using embryonic and tissue stem cells gene sets (Bhattacharya *et al*, 2004; Wong *et al*, 2008).

B Heat-map showing the scaled expression levels (z-score) of self-renewal core genes (Soucie *et al*, 2016) in Maf-DKO macrophages treated or not with NAM for 1 or 10 h.

C Quantitative PCR for the expression of c-Myc, Klf2 and Klf4 in Maf-DKO macrophages treated for the indicated times with 10 mM NAM. Average values of three independent experiments normalized to HPRT. Error bars indicate the standard error of the mean. Each condition was done in duplicate.

D BubbleGUM analysis on microarray samples of Maf-DKO macrophages treated or not with NAM for 1 or 10 h using Myc gene set data from hallmark, canonical pathways and chemical and genetic perturbations collections of the Broad Institute MSig database.

Although the SIRT1 homologue SIR2 has originally been characterized as a histone deacetylase enzyme, it has been subsequently shown that SIRT1 can also deacetylate a wide range of

signalling molecules, including transcription factors such as Myc (Haigis & Sinclair, 2010), which might explain the strong effect on the self-renewal gene network. For example, SIRT1-dependent

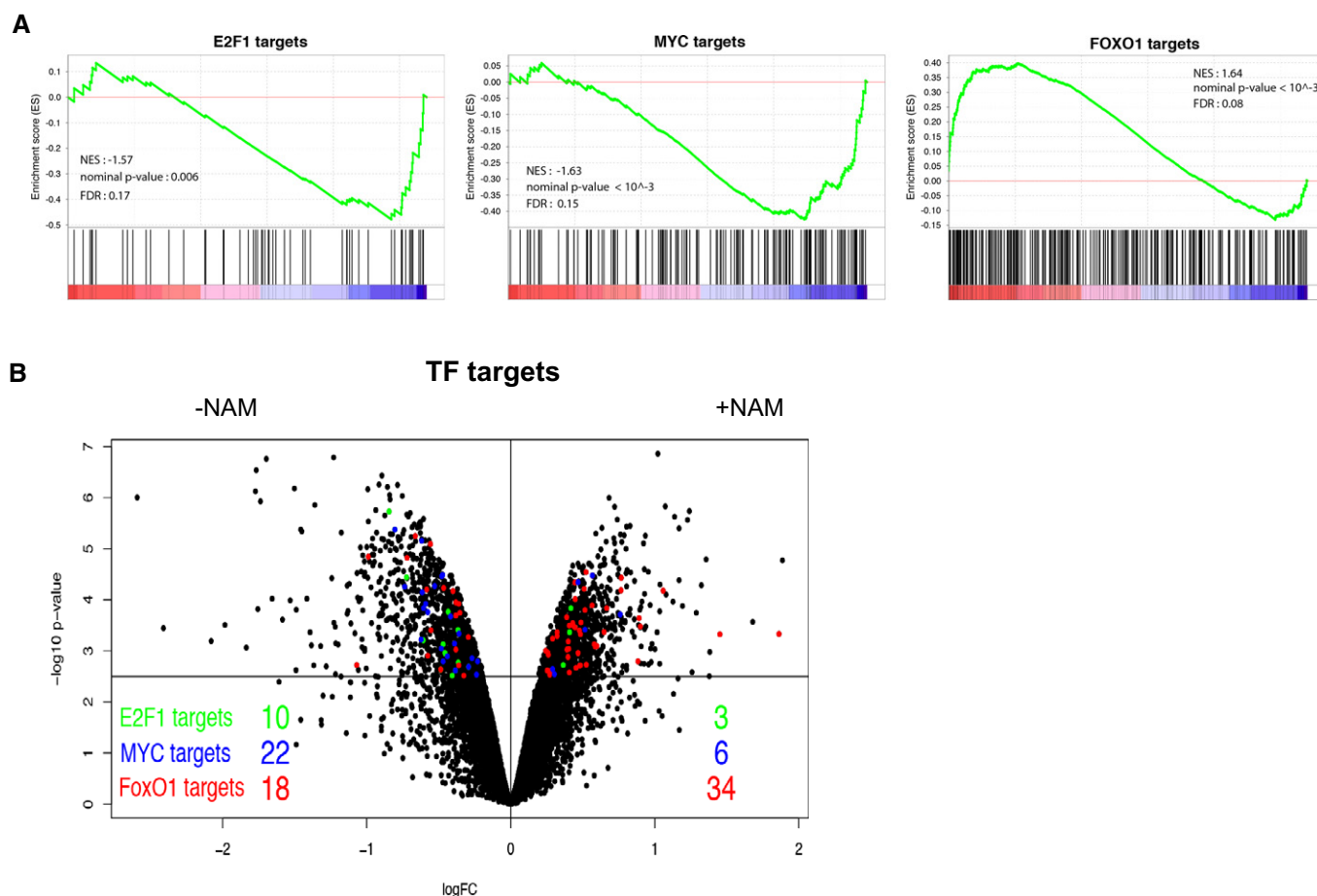


Figure 8. NAM-mediated SIRT1 inhibition in macrophages results in reciprocal regulation of E2F1, Myc and FoxOs activities.

A GSEA analysis of untreated versus 10-h NAM-treated Maf-DKO macrophages with E2F1, FoxO1 and Myc transcription factor target gene sets. V\$FOXO1_01; V\$FOXO1_02; V\$E2F_01; V\$MYC_Q2 gene sets used.

B Volcano plot analysis on microarray samples (Maf-DKO cells treated or not with NAM for 10 h) highlighting E2F1, Fox1 and Myc target genes by GSEA (respectively, green, red and blue dots).

deacetylation of Myc has been described to enhance Myc/Max association (Mao *et al*, 2011) and cell proliferation in other cell systems (Mao *et al*, 2011; Marshall *et al*, 2011; Menssen *et al*, 2012). The direct enzymatic activity of SIRT1 on signalling molecules of cell cycle control might similarly affect cell cycle regulation in self-renewing macrophages. SIRT1 can deacetylate RB, the master regulator of the G₁/S transition of the cell cycle (Harbour & Dean, 2000), which inhibits its ability to sequester and inactivate the transcription factor E2F1 (Wong & Weber, 2007). This provides an explanation why in our experiments SIRT1 inhibition prevented E2F phosphorylation and the transcriptional activation of E2F1 gene targets that drive cell cycle progression. FoxO transcription factors have also been shown to be subject to diverse post-translational modifications, including acetylation, that regulate cytoplasmic/nuclear shuttling (Calnan & Brunet, 2008; Webb & Brunet, 2014). Lysine-deacetylation of FoxO factors by SIRT1 has been shown to prevent their transcriptional activity (Motta *et al*, 2004; Kitamura *et al*, 2005). Although E2F1 can activate FoxO gene transcription (Nowak *et al*, 2007), the mechanism of concomitant

sirtuin-induced retention of FoxO factors in an inactive state in the cytoplasm might prevent FoxO-mediated target gene activation and cell cycle arrest in self-renewing macrophages. Consistent with this, we showed that the inhibition of SIRT1 activity induced nuclear accumulation of FoxO1 and target gene activation in Maf-DKO macrophages. Coordinated SIRT1-mediated deacetylation of key signalling molecules like Rb, Myc and FoxO transcription factors thus appears to result in the coordinated activation of cell cycle progression, self-renewal pathways and the inactivation of stress response induced cell cycle arrest.

SIRT3, another member of the sirtuin family, has also been reported to influence stem cell self-renewal in HSCs (Brown *et al*, 2013). Since Inaahzin, an antagonist of SIRT1 but not SIRT3 (Zhang *et al*, 2012), showed a slightly weaker effect than NAM, an inhibitor of both sirtuins, we also tested the effect of SIRT3 shRNA inactivation in Maf-DKO macrophages. We indeed observed a reduction in the colony-forming ability but to a lesser degree than the one observed after SIRT1 depletion (Appendix Fig S6). Since Inaahzin and shRNA inactivation of SIRT1 recapitulated to a large extent the

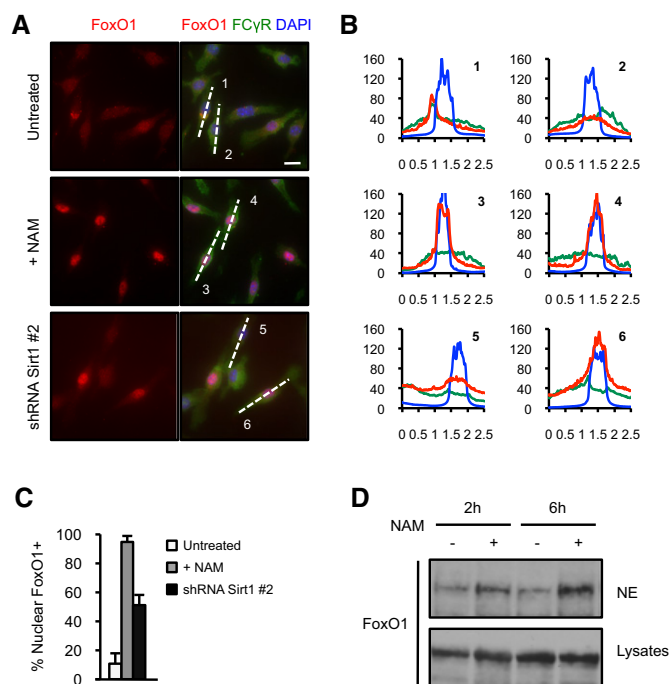


Figure 9. SIRT1 inactivation in macrophages induces nuclear localization of FOXO1.

A Immunofluorescence staining of FoxO1 for nuclear and cytoplasmic localization (red) in untreated Maf-DKO macrophages or after 6-h treatment with 10 mM NAM or after infection with shRNA SIRT1 #2 vector. FcγR (green) immunofluorescence and DAPI (blue) staining was used to define cellular and nuclear perimeters, respectively. The results shown are representative of three independent experiments. Scale bars = 20 μm.

B Line profile analysis with ImageJ software of FoxO1 localization within the cells indicated with dashed line in (A). X- and y-axes represent the fluorescence intensity and the position along the line used for the analyses, respectively (unit = pixels).

C Quantification of nuclear FoxO1 positive cells shown as percentage of total DAPI positive cells. Data shown are pooled from three independent experiments. Error bars indicate the standard error of the mean.

D FoxO1 nuclear localization after SIRT1 inhibition with NAM. Nuclear extracts or total cell extracts were prepared from untreated or SIRT1 inhibitor (10 mM NAM, 20 h) treated Maf-DKO macrophages. Protein blots were incubated with anti-FoxO1 as indicated. Separation of total lysates probed with anti-FoxO1 served as controls.

Source data are available online for this figure.

phenotype of NAM inhibition, this indicates that SIRT1 is the main sirtuin regulator of macrophage self-renewal.

Interestingly, the temporary inhibition of SIRT1 by NAM permits an adapted and short-term restriction of macrophage proliferation without compromising their long-term self-renewal capacity. Since NAM is the amide form of the vitamin B3 that is also taken up with food, diet might have an important impact on macrophage proliferation and homeostasis *in vivo*. The concentration of NAM appears to be critical, with a concentration of 10 mM achieving maximal inhibition of macrophage proliferation in our experiments in culture and *in vivo*. In human patients, a serum concentration of NAM ranging from 2 to 10 mM was measured after buccal absorption (Spector, 1987). The range of reported normal physiological concentration of NAM in rodents (0.9–2.2 mM) already showed moderate effects on

macrophage proliferation in our experiments but lies well below the value of full inhibition (10 mM). This suggests that the normal concentrations of NAM are just at the sensitivity threshold where both reduction and increase of NAM would have significant effects on macrophage proliferation. This might be relevant and important for potential pharmacological intervention.

Here, we demonstrated effects of SIRT1 inhibition on macrophage self-renewal in several prototypic macrophage populations, including alveolar and peritoneal macrophages *in vivo*. Although we have not specifically analysed other resident macrophage populations such as microglia, Kupffer cells or Langerhans cells, the observed broad effect of SIRT1 inhibition suggests that SIRT1 activity might also be more generally important in other macrophage subtypes. Given that self-renewal has been observed in many macrophage populations, NAM and SIRT1 activity might thus be relevant for multiple disease conditions with important macrophage contribution and macrophage proliferation. For example, vitamin B3 deficiency or malnutrition for tryptophan, a precursor for *in vivo* synthesis of nicotinic acid and NAM, leads to pellagra or related symptoms including weight loss and diarrhoea. This is associated with massive intestinal infiltration of inflammatory cells (Hashimoto *et al*, 2012) and production of the pro-inflammatory cytokines IL-22 and IL-17 cytokines. In this system, inflammation could be reduced by administration of tryptophan or NAM. Although the target cell of this effect was not described, it is interesting to speculate that the inflammatory phenotype might involve deregulated proliferation of pro-inflammatory monocytes/macrophage and that its repression by NAM might be beneficial. Atherosclerosis is another example of a pro-inflammatory condition where macrophage proliferation in the arterial wall drives pathogenic macrophage accumulation (Robbins *et al*, 2013). NAM-mediated SIRT1 inhibition and repression of excessive proliferation of macrophages might also be beneficial under these conditions. Consistent with this, genetic myeloid deletion of FoxO factors increased monocyte numbers and exacerbated atherosclerotic lesions (Feinberg, 2013; Tsuchiya *et al*, 2013). Targeting the SIRT1/FoxOs pathway could thus be promising strategy in these pathologies by suppressing proliferation of inflammatory macrophages and monocytes. Finally, the control of SIRT1 activity on macrophage proliferation could be relevant for neuroinflammation and neurodegenerative diseases, such as Alzheimer disease or multiple sclerosis, where microglia, the macrophages of the central nervous system (CNS), have been shown to be highly disease relevant (Perry *et al*, 2010; Prinz *et al*, 2011; Prinz & Priller, 2014; Gomez-Nicola & Perry, 2016). Microglia cells can undergo massive proliferation and expansion during diverse CNS pathologies and in response to genetic ablation or injury (Ajami *et al*, 2007; Prinz *et al*, 2011; Waisman *et al*, 2015; Gomez-Nicola & Perry, 2016), but it has not been conclusively determined whether microglia proliferation is beneficial or detrimental in various disease settings.

Conversely, reduced macrophage proliferation capacity might be relevant to various ageing processes. Declining self-renewal of stem cells with age has been linked to the decreasing capacity for tissue regeneration and general age-related tissue attrition in multiple organ systems (Oh *et al*, 2014). The role of sirtuins in longevity mechanisms might thus be related to their more recently described role in stem cell self-renewal, which has been demonstrated for SIRT3 in HSCs (Brown *et al*, 2013) and for SIRT1 in a

variety of tissue specific (Rathbone *et al*, 2009; Yuan *et al*, 2012; Singh *et al*, 2013; Rimmele *et al*, 2014; Niu *et al*, 2016; Zhang *et al*, 2016a) and embryonic stem cells (Han *et al*, 2008; Calvanese *et al*, 2010; Saunders *et al*, 2010). The yeast sirtuin homologue sir2 was originally shown to extend replicative life span of yeast, and overexpression of the metazoan homologues had been reported to extend life span in worms and flies (Tissenbaum & Guarente, 2001; Kenyon, 2005). Although these earlier claims remained contested, recent findings tend to resolve many discrepancies (Guarente, 2013). Sirtuins mediate effects of caloric restriction that results in life span extending metabolic changes and several tissue-specific SIRT1-deficient mouse models indicate that SIRT1 can impact on age-related physiological decline (Boutant & Canto, 2014). Furthermore increased life span was observed upon brain-specific overexpression of SIRT1 (Satoh *et al*, 2013) or repletion of the SIRT substrate NAD⁺ in old mice that improved tissue stem cell function in a SIRT1-dependent fashion (Zhang *et al*, 2016a).

SIRT1 activity on histone or non-histone substrates affects multiple cellular processes relevant to ageing, such as inflammation, apoptosis, adipogenesis, autophagy, glucose homeostasis, genome stability, telomere length, DNA repair, stem cell activity and stress resistance. Among the non-histone substrates of sirtuins, FoxO transcription factors are known to affect longevity and health span via several mechanisms (Martins *et al*, 2016). Besides their role in cell cycle arrest, FoxO transcription factors act as oxidative sensors and regulate intracellular redox status by modulating the expression of anti-oxidant enzymes and DNA damage responses (Charitou & Burgering, 2013; Klotz *et al*, 2015) as well as autophagy and mitophagy (Pietrocola *et al*, 2013; Webb & Brunet, 2014). In *C. elegans*, the Sirtuin gene *sir-2.1* regulates life span extension by deacetylation of the DAF-16 protein, a FoxO family member (Berdichevsky *et al*, 2006). Under stress conditions, such as deprivation of growth factors, cells react by inducing nuclear localization of FoxO proteins, leading to (G₁-S) cell cycle arrest by p27 and p21 activation and cyclin D gene inhibition (Medema *et al*, 2000; Schmidt *et al*, 2002; Seoane *et al*, 2004). In the murine hematopoietic system, FoxO proteins have been demonstrated to restrict proliferation potential and repopulating activity of HSCs (Tothova *et al*, 2007). Myeloid-specific FoxO triple knockout mice exhibited increased granulocytes–macrophages progenitor proliferation, monocytosis and increased proliferation with decreased apoptosis of cultured peritoneal macrophages (Tsuchiya *et al*, 2013). Furthermore, a direct link has been described between FoxO transcription factors and the Akt kinase that is part of a shared gene network regulating self-renewal both in macrophages and ES cells (Soucie *et al*, 2016). Several mitogenic stimuli act by Akt-dependent phosphorylation, nuclear exclusion and degradation of FoxO proteins (Biggs *et al*, 1999; Accili & Arden, 2004) and Akt signalling is important in macrophage proliferation (Ruckerl *et al*, 2012). The link between sirtuins and this pathway is further supported by our study, where in proliferating macrophages SIRT1 inhibition induced nuclear localization of FoxO transcription factors, up-regulation of FoxO targets, cell cycle arrest and down-regulation of Akt.

It has been proposed that the attrition of stem cell activity and regenerative capacity is a hallmark of ageing (Oh *et al*, 2014). Here, we have demonstrated that SIRT1 activity is not only required for

self-renewal in stem cells but also in macrophages. Some tissue resident macrophage populations are long-lived, have self-renewal capacity (Sieweke & Allen, 2013) and have recently been demonstrated to be required for tissue regeneration (Godwin *et al*, 2013; Aurora *et al*, 2014; Petrie *et al*, 2014). It is therefore tempting to speculate that the general life and health span extending activities of sirtuins might not only depend on counteracting ageing in stem cells but also in macrophages.

Materials and Methods

Cells and culture media

Maf-DKO macrophages were cultured in DMEM (Life Technologies®/Invitrogen) containing 10% heat-inactivated FCS (GE Healthcare/PAA, A15-101), 1% penicillin–streptomycin, 1% sodium pyruvate and 1% of L-glutamine (Life Technologies®/Invitrogen), supplemented with 20% supernatant of M-CSF producing L-929 cells (L-cell sup; Stanley, 1985). Maf-DKO macrophages were cultured with medium changes every 2–3 days. For functional assays, Maf-DKO macrophages were seeded in six-well plates and cultured overnight in M-CSF conditioned medium at a density of 2×10^5 cells/well. The morning after, cells were stimulated with fresh medium supplemented or not with NAM (Sigma-Aldrich, N0636) for 48 h. WT BMM macrophages were differentiated from total mouse bone marrow for 15 days in macrophage growth medium (L-cell sup), selecting for adherent cells every 4 days. rtTA macrophages were differentiated from total rtTA mouse bone marrow (The Jackson Laboratory: Gt(ROSA)26Sor^{tm1(rtTA**M2*)Jae}) for 5 days in macrophage growth medium (L-cell sup) and then infected with SIRT1 expressing retrovirus. For culture of AM, alveolar lavages were pooled from ten 1 ml 37°C BAL washes (PBS without Mg²⁺/Ca²⁺, 2 mM EDTA, 2% FBS; GE Healthcare) per mouse and stored on ice. RBC lysis was then performed at room temperature (RT) for 3 min (RBC Lysis Buffer, Invitrogen). Cells were plated at a density of 1.1 million cells per 10 cm bacterial petri dish in complete medium (RPMI, 10% FCS, 1% Pen/Strep, 1% Pyruvate, 1% Glutamate) supplemented with 1% GM-CSF supernatant from J558L cells transfected with murine GM-CSF cDNA (a kind gift of Dr. D. Gray, London, UK).

Peritoneal and alveolar macrophages stimulation and isolation

Six- to eight-week-old female C57BL/6 mice were obtained from Janvier laboratories. All mouse experiments were performed under specific pathogen-free conditions in accordance with institutional guidelines. For baseline proliferation measurement of alveolar and peritoneal macrophages, mice were injected into the peritoneal cavity with either PBS or NAM (10 mM in 200 µl for PM, 20 mM in 200 µl for AM; Sigma-Aldrich N0636) or Inauhzin (30 mg/kg; Calbiochem 566332). NAM and PBS control injections were repeated after 24 h. The proliferation capacity of alveolar and peritoneal macrophages was assessed after 48 h. Peritoneal macrophages were harvested by peritoneal wash with PBS containing EDTA (2 mM), incubated with Fc receptor blocking antibody (clone 2.4 G2, BD 553142) and stained for FACS analysis using the following antibodies: anti-B220 (Clone RA3-6B2, BioLegend

103221); anti-Ly6C (Clone AL-21, BD 553104); anti-F4:80 (Clone BM8, BioLegend 123141); anti-CD64 (Clone X54-5/7.1, BioLegend 139308); anti-CD11b (Clone HL3, BD 563057); and anti-Tim4 (Clone 54 (RMT4-54), Ebioscience 12-5866-80). Zombie UV Fixable Viability Kit (BioLegend 423108) was used to stain dead cells. Whole lungs were macerated and incubated with 1 mg/ml Collagenase-2 (Worthington Biochemical Corporation CLS-2) and 0.15 mg/ml DNaseI (Roche 10104159001) at 37°C for 30 min during constant agitation. The resulting cell suspension was filtered through a 70-µm mesh and erythrocytes were removed by ACK lysis. Cells were incubated with Fc receptor blocking antibody (clone 2.4 G2, BD 553142) and stained for FACS analysis using the following antibodies: anti-SiglecF (Clone E50-2440, BD 552126) and anti-CD11c (Clone N418, BioLegend 117349). Zombie UV Fixable Viability Kit (BioLegend 423108) was used to stain dead cells. After extracellular staining, permeabilization was performed using BD Cytofix/Cytoperm™ solution. The proliferation capacity of alveolar and peritoneal macrophages was assessed using antibody directed against Ki67 (Clone 16A8, BioLegend 652411) or a corresponding isotype control (Rat IgG2a kappa Isotype Ctrl, BioLegend 400549). For induced M-CSF peritoneal macrophage proliferation, mice were injected into the peritoneal cavity with either PBS or pig CSF1-Fc (1 µg/g body weight; a kind gift from David Hume; Gow *et al*, 2014) supplemented with or without NAM (10 mM, Sigma-Aldrich N0636). NAM and PBS control injections were repeated after 24 h. The proliferation capacity of M-CSF-induced resident peritoneal macrophages was assessed after 48 h, with intra-peritoneal injection of EdU (5-ethynyl-2'-deoxyuridine, 2 mg/g body weight; Life Technologies) 4 h before analysis. Cells were harvested by peritoneal wash with PBS containing EDTA (2 mM) and stained with fluorochrome-conjugated antibodies. Detection of EdU incorporation was performed using the Click-iT® Plus EdU Flow Cytometry Assay Kit (Life Technologies) following the manufacturers' instructions. Cells were acquired on a LSRII UV Flow Cytometer DIVA™ software (both BD) and analysed using FlowJo software (TreeStar).

sgRNA viral vector infections

sgRNAs (designed by CRISPRGold; Chu *et al*, 2016; targeting Sirt1) were cloned into BbsI sites of the pKLV-U6gRNA(BbsI)-PGKpuro-2ABFP vector (Addgene #50946). Lentiviral particles were produced by the SFR facility (Lyon, France). Alveolar macrophages were harvested by bronchoalveolar lavage from Rosa26-Cas9p2aGFP transgenic mice (Chu *et al*, 2016) and transduced with lentiviral supernatant for 4 h. After 1 day, transduced cells were selected with 2 µg/ml puromycin for 2 days. Selected alveolar macrophages were subjected to fluorescence-activated cell sorting (FACS) to enrich for BFP^{hi} macrophages and cultured in absence of puromycin.

shRNA viral vector infections

Plasmids encoding shRNA-targeting SIRT1 (TRCN0000306512; TRCN0000326966) and SIRT3 (TRCN0000306513; TRCN00000039331) were purchased from Sigma, while the plasmid encoding shRNA-targeting LacZ (TRCN0000072226) was obtained from The RNAi Consortium (TRC; Broad Institute, Cambridge, MA, USA;

Moffat *et al*, 2006). High-titer lentivirus encoding shRNA-targeting genes of interest were produced by the SFR facility (Lyon, France) by triple co-transfection of plasmids harbouring the packaging construct, the transfer vector (Amit *et al*, 2009) and the envelope-expressing construct into producer cells using calcium chloride transfection. Virus was concentrated after transfection, and viral supernatants were harvested and stored at −80°C. Prior to infection, Maf-DKO macrophages were seeded in 6-well plate and cultured overnight at a density of 5×10^5 cells/well. The morning after, viral supernatants were incubated with 8 µg/ml of polybrene for 90 min at 37°C, 5% CO₂ and a volume of 4 ml/well/infection was used to replace media on Maf-DKO macrophages. Cells were transduced by spin infection in virus-containing medium, by centrifugation at 1,200 g for 2.5 h at 25°C. Viral supernatants were removed immediately after spin infection and replaced with medium, and Maf-DKO cells were then further incubated at 37°C, 5% CO₂ for 48 h prior to harvesting and divided into fractions for knock down efficiency test (qRT-PCR and immunostaining for the target genes), and functional colony formation assay.

SIRT1 overexpression in rtTA BMMs

Puro^r was replaced by GFP in pRetroX-tight-Pur (Clontech, 632104). The pRetroX-Sirt1-PGK-GFP was used for inducible expression of SIRT1 by doxycycline administration (Sigma). Phoenix[®] E cells were used for production of retroviral particles following the protocol of the Laboratory of Nolan (www.stanford.edu/group/nolan/) 48 h after transfection. Phoenix cells were cultured in M-CSF conditioned medium (L-cell sup), in a 32°C incubator overnight, and supernatant was used to infect rtTA BMMs cells plated at 5×10^5 cells/well in six-well dish 1 day before infection. Cells were infected by two spin infections in virus-containing medium (supplemented with 8 µg/ml of Polybrene), by means of centrifugation at 1,200 g for 2 h at 32°C after 5 days of differentiation. Freshly after the last infection round, the viral supernatant was replaced by fresh medium. Five days after infection, cells were FACS analysed for Ki67 as described for *in vivo* assays. All the infection steps are performed with supplement of 500 ng/ml doxycycline for the induced conditions.

Colony assays

500 Maf-DKO macrophages were plated in semi-solid methylcellulose medium (M3231, StemCell™ Technology) containing 100 ng/ml of recombinant murine M-CSF (Peprotech) and supplemented with different concentrations of NAM (Sigma-Aldrich, N0636), 1 µM Inauhzin (Merck Chemicals, 566332), 1 µM Olaparib (Euromedex, AZD2281) or 200 µM NMN (Sigma-Aldrich, N3501). Number and types of colonies were scored between 14 days after plating. Transduced alveolar macrophages were plated in duplicates at a density of 10,000 cells per 1 ml of MethoCult medium (M3231, Stem Cell™ Technologies), with the addition of 100 ng/ml of recombinant GM-CSF (Peprotech). The number of CFUs was counted on day 14 after plating.

Cell cycle analysis

Maf-DKO macrophages were harvested with trypsin-EDTA (Life Technologies[®]/Invitrogen), transferred to a V-bottomed tube,

washed once with PBS, fixed with 70% ethanol for 1 h at 4°C, washed twice with PBS, treated with 100 µg of RNase A for 30 min at 37°C, washed once with PBS, and finally stained with 20 µg of propidium iodide (Sigma-Aldrich, P4864) in PBS. Cells were analysed upon FACS acquisition using linear amplification setup. For BrdU incorporation assay, Maf-DKO macrophages were cultured as described earlier. During the last 24 h of culture, cells were supplemented with 10 µM BrdU (BD) and incubated at 37°C. BrdU incorporation was detected using the BD BrdU Flow Cytometry® Kit (BD) according to manufacturer's protocol. Briefly, after collection with trypsin-EDTA, cells were fixed, permeabilized and washed. DNA was digested with DNase provided with the kit and anti-BrdU antibody conjugated to FITC was added to the cells. For FACS acquisition, Maf-DKO macrophages were resuspended in FACS medium (0.5% FCS and 1 mM EDTA in PBS), at a concentration of 1×10^6 – 1×10^7 cells/ml. For Ki67 intracellular staining, cells were harvested and treated as for BrdU staining but treated with an antibody directed against Ki67 (Clone 16A8, BioLegend 652411) or a corresponding isotype control (Rat IgG2a kappa Isotype Ctrl, BioLegend 400549). Cells were analysed on FACSCanto II (BD) or LSRII and by FlowJo software (Tree Star).

Immunohistochemistry

Maf-DKO macrophages were seeded in LabTek-II chamber slides (Nunc) at 1×10^5 cells/well and cultured overnight. The next day, cells were stimulated with fresh medium supplemented or not with 10 mM NAM for 48 h. Cells were fixed immediately with PBS/4% formaldehyde for 10 min at RT. After fixation, samples were washed twice in PBS, and then incubated in PBS/0.25% Triton X-100 for 10 min. Cells were then incubated for 30 min in PBS/2% BSA/1:100 anti-CD16/32 (BD, clone 2.4G2) for blocking non-specific interaction and then overnight with the primary antibodies against Ki67 (Dako, M7249; 1:50), activated Caspase-3 (Cell Signaling Technology®, #9644; 1:200), SIRT1 (Cell Signaling Technology®, #8469; 1:100), phospho-E2F1 (Abcam, ab55325; 1:200), FoxO1 (Cell Signaling Technology®, #2880; 1:200) or FoxO3 (Cell Signaling Technology®, #2497; 1:100). Samples were washed twice in PBS and then incubated 45 min with AlexaFluor® dye conjugated secondary antibodies (Molecular Probes®/Invitrogen; 1:100). Finally, cells were washed twice in PBS, dried and mounted with ProLong Gold antifade/DAPI reagent (Molecular Probes®/Invitrogen). Photomicrographs were taken with multi-fluorescence Zeiss Axioplan 2 microscope and acquired with SmartCapture 2 software. For positive controls of apoptosis, sections of pancreas from streptozotocin (STZ)-treated mice (McEvoy *et al.*, 1984) were used. In short, for multi-low-dose streptozotocin (STZ) experiments, adult males (6- to 8-week-old) were fasted for 4 h prior to i.p. injection with 40 mg/kg of body weight of STZ prepared in Na-citrate buffer 0.1 mol/l (pH 4.5) over five consecutive days and diabetes was monitored for 2 weeks after the last injection. Pancreases were fixed overnight at 4°C in 4% formalin (v/v) and for 1–2 days in sucrose 20% (w/v) at 4°C, before embedding in Tissue Tek (OCT Compound, Sakura Finetek Europe, Zoeterwoude, the Netherlands). Whole pancreases were serially sectioned and stained as described above. Percentage of positive stained cells was evaluated using Cell Counter Plug-in of ImageJ software.

Preparation of cell extracts and nuclear extracts

Cells were washed twice with phosphate-buffered saline (PBS) and resuspended in lysis buffer [20 mM HEPES pH 7.8, 150 mM NaCl, 1 mM EDTA pH 8, 10 mM MgCl₂, 0.5% NP40, 10% Glycerol, 20 U/ml Benzonase (Sigma), protease inhibitor cocktail (Roche), 1 mM DTT, 1 mM PEFA bloc (Böhringer), 1 µM trichostatin A (TSA), 10 mM NAM (Sigma), 10 mM Na-butyrate (Sigma)]. After incubation on ice for 30 min cell debris was removed by centrifugation at 16,000 g for 20 min. Nuclear extracts were prepared as described (Schreiber *et al.*, 1989). Briefly, PBS-washed cells were incubated with hypotonic buffer (20 mM HEPES pH 7.8), 1.5 mM MgCl₂, 10 mM KCL, protease inhibitor cocktail, 1 mM DTT, 1 mM PEFA, 1 µM trichostatin A (TSA), 10 mM NAM, 10 mM Na-butyrate), 0.1% NP40 was added and the cytoplasmic fraction was removed by short centrifugation. Nuclei were resuspended in hypertonic buffer (20 mM HEPES pH 7.8, 400 mM NaCl, 1.5 mM MgCl₂, 0.2 mM EDTA pH8, 20% glycerol, protease inhibitor cocktail (Roche), 1 mM DTT, 1 mM PEFA bloc, 1 µM trichostatin A (TSA), 10 mM NAM, 10 mM Na-butyrate), incubated on rocker on ice for 30 min, and supernatants were recovered as nuclear extracts after centrifugation at 16,000 g for 20 min. For Western blotting experiments, the primary antibodies used were Anti-FoxO1 (Cell Signaling #C29H4), Anti-H3 (Abcam #ab 1791) and Anti-H3 K9ac (Abcam #ab 10812).

RNA extraction and quantitative RT-PCR

Lentivirally infected Maf-DKO macrophages were seeded in six-well plates and cultured overnight at a density of 2×10^5 cells/well. The morning after, cells were stimulated with fresh medium for 4 h prior to RNA isolation. RNAs were extracted using Qiagen RNeasy Mini Kit (Qiagen). 500 ng of RNA from each sample was used for Reverse Transcription (Superscript II®, Invitrogen). Oligo(dT) was used to perform reverse transcription. For quantitative real-time PCR, we used Power SYBR Green PCR Master Mix and a 7,500 Fast Real-Time PCR System sequence detection system (both Applied Biosystem), following the manufacturer's instructions. Amplification of the cDNA was performed by using primers for HPRT (5'-GGCCCTC TGTGTGCTCAAG-3', Fwd; 5'-CTGATAAAATCTACAGTCATAGGAA TGGA-3', Rev), sirt1 (5'-AACAATTCCTCCACCTGAGC-3', Fwd; 5'-TCCCACAGGAGACAG AAACC-3', Rev), sirt3 (5'-ACAGTACATGC ACGGTCTG-3', Fwd; 5'-ACACAATGTCGGGTTTCACA-3', Rev), c-myc (5'-CAGAGGAGGAACAACGAGCTGAAGCGC-3', Fwd; 5'-TTAT GCACCAGAGTTTCGAAGCTGTTTCG-3', Rev), klf2 (5'-ACCAAGAGC TCGCACCTAAA-3', Fwd; 5'-GTGGCACTGAAAGGGTCTGT-3', Rev), klf4 (5'-ATGGTCAAGTTCACAGCAAG-3', Fwd; 5'-GGGCATGTTCAA GTTGATT-3', Rev).

Microarray analysis

Maf-DKO macrophages were seeded in six-well plates and cultured overnight at a density of 2×10^5 cells/well. The next day, cells were stimulated with fresh medium supplied (or not) with 10 mM NAM for 1 or 10 h prior to RNA isolation. Total RNA of Maf-DKO cells ($n = 3$ biological replicates for each sample) was extracted as described earlier. The quality of RNA was assessed using Agilent 2100 Bioanalyzer using Eukaryote Total RNA Nano Chip platform

(Agilent Technologies). The extracted RNA had a RIN > 9. For each sample, 200 ng of RNA was processed by the Microarray and Sequencing Platform (IGBMC, Strasbourg, France), and the obtained biotinylated cDNAs were hybridized on Mouse Gene 1.0 ST array Chip (Affymetrix). Normalization of raw Affymetrix expression data (extracted from CEL files) was performed by Robust Multi-chip Analysis (Irizarry *et al*, 2003) through Bioconductor (release 2.9) in the R statistical environment (version 2.14) via the Affy package. Probe sets over a normalized expression value of 6 (log2 scale) in at least one sample across all arrays were considered as expressed and were included in the analysis. At the end, 15,363 probes were kept for the subsequent analysis. In order to select the regulated probes between conditions, LimMA package (Linear Model for Microarray Data) using an empirical Bayes method was used (Smyth, 2004). Genes having an adjusted *P*-value inferior to 0.05 were considered as regulated. The Gene Set Enrichment Analysis (GSEA) method from the Massachusetts Institute of Technology (<http://www.broad.mit.edu/gsea>) is based on a Kolmogorov–Smirnov test (Subramanian *et al*, 2005). This method was used to statistically test whether a set of genes of interest was distributed randomly in the large list of genes (corresponding to the 15,363 probes) sorted on the basis of the log difference of their expression level between “10 h NAM-treated” and “no NAM control” culture conditions. Transcription factor targets gene sets (C3) from MSigDB Collections (TFT collection gene sets; <http://software.broadinstitute.org/gsea/msigdb/genesets.jsp?collection=TFT#>) were used for these analyses. Each gene set of interest (V\$FOXO1_01; V\$FOXO1_02; V\$FOXO3_01; V\$FOXO4_01; V\$FOXO4_02; V\$E2F_01; V\$USF_C; V\$MYC_Q2; V\$MYC_MAX_01; V\$MYC_MAX_02) contains genes that share a transcription factor-binding site defined in the TRANSFAC database (version 7.4, <http://www.gene-regulation.com>). For heat-map representation, multiple probe sets corresponding to each gene were aggregated by their median expression value. BubbleGUM is an open-source software performing numerous GSEA analysis with multiple testing correction (Spinelli *et al*, 2015). The Reactome pathway database (<http://www.reactome.org>) was chosen as gene set compendium for its accuracy to describe cell cycle phases and events. Microarray data are available at (<http://www.ncbi.nlm.nih.gov/geo/query/acc.cgi?acc=GSE60187>).

Expanded View for this article is available online.

Acknowledgements

We thank David Hume, The Roslin Institute, University of Edinburgh, for the CSF1-Fc reagent and Klaus Rajewsky, MDC, Berlin, for Rosa26-Cas9p2aGFP transgenic mice. We are thankful to Gregory Gimenez, Van Trung Chu and Robin Graf for technical advice and to Sandrine Sarrazin for mouse colony management. We thank the Centre d'Immunologie de Marseille-Luminy (CIML) mouse house and cytometry facilities and Gisèle Froment, Didier Nègre and Caroline Costa from the lentivectors production facility/SFR BioSciences Gerland-Lyon Sud (UMRS3444/US8). We acknowledge the PICSL imaging facility of the CIML (ImagImm), member of the national infrastructure France-BioImaging supported by the French National Research Agency (ANR-10-INBS-04). The work was supported by institutional grants from INSERM, CNRS and Aix-Marseille University to the CIML and grants to MHS from the Volkswagen Stiftung (I/79 994-996), “Agence nationale de la Recherche” (ANR-11-BSV3-0026), Fondation pour la Recherche Médicale (DEQ. 20071210559 and DEQ. 20110421320) and the European Research Council (ERC) under the European

Union's Horizon 2020 research and innovation programme (grant agreement number 695093 MacAge). FI was supported by a fellowship from the Fondation pour la Recherche Médicale (FDT20111223609). MHS is a BIH-Einstein fellow and INSERM-Helmholtz group leader.

Author contributions

FI designed and performed the majority of experiments, analysed data, contributed to writing of the article and prepared figures. JM analysed bioinformatics data. SVA performed *in vivo* proliferation assays and viral vector infections. CJB and JF performed CRISPR/Cas9 and CFC assays. WC provided technical help for *in vivo* experiments, viral vector infections, cell culture and RT-QPCR. EK-L performed biochemical acetylation and nuclear localization assays and RG performed some of the *in vivo* proliferation assays. PP provided technical help. AL provided constructive discussions. CB contributed to experiments, analysed data, designed and supervised the study, and wrote the article. MHS designed and supervised the study, analysed data and wrote the article.

Conflict of interest

The authors declare that they have no conflict of interest.

References

- Accili D, Arden KC (2004) FoxOs at the crossroads of cellular metabolism, differentiation, and transformation. *Cell* 117: 421–426
- Ajami B, Bennett JL, Krieger C, Tetzlaff W, Rossi FM (2007) Local self-renewal can sustain CNS microglia maintenance and function throughout adult life. *Nat Neurosci* 10: 1538–1543
- Amit I, Garber M, Chevrier N, Leite AP, Donner Y, Eisenhaure T, Guttman M, Grenier JK, Li W, Zuk O, Schubert LA, Birditt B, Shay T, Goren A, Zhang X, Smith Z, Deering R, McDonald RC, Cabili M, Bernstein BE *et al* (2009) Unbiased reconstruction of a mammalian transcriptional network mediating pathogen responses. *Science* 326: 257–263
- Aurora AB, Porrello ER, Tan W, Mahmoud AI, Hill JA, Bassel-Duby R, Sadek HA, Olson EN (2014) Macrophages are required for neonatal heart regeneration. *J Clin Invest* 124: 1382–1392
- Avalos JL, Bever KM, Wolberger C (2005) Mechanism of sirtuin inhibition by nicotinamide: altering the NAD(+) cosubstrate specificity of a Sir2 enzyme. *Mol Cell* 17: 855–868
- Aziz A, Soucie E, Sarrazin S, Sieweke MH (2009) MafB/c-Maf deficiency enables self-renewal of differentiated functional macrophages. *Science* 326: 867–871
- Bain CC, Hawley CA, Garner H, Scott CL, Schridde A, Steers NJ, Mack M, Joshi A, Williams M, Mowat AM, Geissmann F, Jenkins SJ (2016) Long-lived self-renewing bone marrow-derived macrophages displace embryo-derived cells to inhabit adult serous cavities. *Nat Commun* 7: ncomms11852
- Barthel A, Schmoll D, Unterman TG (2005) FoxO proteins in insulin action and metabolism. *Trends Endocrinol Metab* 16: 183–189
- Berdichevsky A, Viswanathan M, Horvitz HR, Guarente L (2006) *C. elegans* SIR-2.1 interacts with 14-3-3 proteins to activate DAF-16 and extend life span. *Cell* 125: 1165–1177
- Bhattacharya B, Miura T, Brandenberger R, Mejido J, Luo Y, Yang AX, Joshi BH, Ginis I, Thies RS, Amit M, Lyons I, Condie BG, Itskovitz-Eldor J, Rao MS, Puri RK (2004) Gene expression in human embryonic stem cell lines: unique molecular signature. *Blood* 103: 2956–2964
- Biggs WH III, Meisenhelder J, Hunter T, Cavenee WK, Arden KC (1999) Protein kinase B/Akt-mediated phosphorylation promotes nuclear exclusion of the

- winged helix transcription factor FKHR1. *Proc Natl Acad Sci USA* 96: 7421–7426
- Bitterman KJ, Anderson RM, Cohen HY, Latorre-Esteves M, Sinclair DA (2002) Inhibition of silencing and accelerated aging by nicotinamide, a putative negative regulator of yeast sir2 and human SIRT1. *J Biol Chem* 277: 45099–45107
- Boutant M, Canto C (2014) SIRT1 metabolic actions: integrating recent advances from mouse models. *Mol Metab* 3: 5–18
- Brown K, Xie S, Qiu X, Mohrin M, Shin J, Liu Y, Zhang D, Scadden DT, Chen D (2013) SIRT3 reverses aging-associated degeneration. *Cell Rep* 3: 319–327
- Calnan DR, Brunet A (2008) The FoxO code. *Oncogene* 27: 2276–2288
- Calvanese V, Lara E, Suarez-Alvarez B, Abu Dawud R, Vazquez-Chantada M, Martinez-Chantar ML, Embade N, Lopez-Nieva P, Horrillo A, Hmadcha A, Soria B, Piazzolla D, Herranz D, Serrano M, Mato JM, Andrews PW, Lopez-Larrea C, Esteller M, Fraga MF (2010) Sirtuin 1 regulation of developmental genes during differentiation of stem cells. *Proc Natl Acad Sci USA* 107: 13736–13741
- Chang HC, Guarente L (2014) SIRT1 and other sirtuins in metabolism. *Trends Endocrinol Metab* 25: 138–145
- Charitou P, Burgering BM (2013) Forkhead box(O) in control of reactive oxygen species and genomic stability to ensure healthy lifespan. *Antioxid Redox Signal* 19: 1400–1419
- Cheng HL, Mostoslavsky R, Saito S, Manis JP, Gu Y, Patel P, Bronson R, Appella E, Alt FW, Chua KF (2003) Developmental defects and p53 hyperacetylation in Sir2 homolog (SIRT1)-deficient mice. *Proc Natl Acad Sci USA* 100: 10794–10799
- Chu VT, Graf R, Wirtz T, Weber T, Favret J, Li X, Petsch K, Tran NT, Sieweke MH, Berek C, Kuhn R, Rajewsky K (2016) Efficient CRISPR-mediated mutagenesis in primary immune cells using CrispRGold and a C57BL/6 Cas9 transgenic mouse line. *Proc Natl Acad Sci USA* 113: 12514–12519
- Chung S, Yao H, Caito S, Hwang JW, Arunachalam G, Rahman I (2010) Regulation of SIRT1 in cellular functions: role of polyphenols. *Arch Biochem Biophys* 501: 79–90
- Davies LC, Rosas M, Smith PJ, Fraser DJ, Jones SA, Taylor PR (2011) A quantifiable proliferative burst of tissue macrophages restores homeostatic macrophage populations after acute inflammation. *Eur J Immunol* 41: 2155–2164
- Davies LC, Rosas M, Jenkins SJ, Liao CT, Scurr MJ, Brombacher F, Fraser DJ, Allen JE, Jones SA, Taylor PR (2013) Distinct bone marrow-derived and tissue-resident macrophage lineages proliferate at key stages during inflammation. *Nat Commun* 4: 1886
- Ekblad T, Schuler H (2016) Sirtuins are unaffected by PARP inhibitors containing planar nicotinamide bioisosteres. *Chem Biol Drug Des* 87: 478–482
- Fagan R, Flint KJ, Jones N (1994) Phosphorylation of E2F-1 modulates its interaction with the retinoblastoma gene product and the adenoviral E4 19 kDa protein. *Cell* 78: 799–811
- Feinberg MW (2013) OutFOXing myeloid cells in atherosclerosis with FoxOs. *Circ Res* 112: 978–982
- Frescas D, Valenti L, Accili D (2005) Nuclear trapping of the forkhead transcription factor FoxO1 via Sirt-dependent deacetylation promotes expression of glucogenetic genes. *J Biol Chem* 280: 20589–20595
- Frye RA (2000) Phylogenetic classification of prokaryotic and eukaryotic Sir2-like proteins. *Biochem Biophys Res Commun* 273: 793–798
- Geissmann F, Manz MG, Jung S, Sieweke MH, Merad M, Ley K (2010) Development of monocytes, macrophages, and dendritic cells. *Science* 327: 656–661
- Gentek R, Molawi K, Sieweke MH (2014) Tissue macrophage identity and self-renewal. *Immunol Rev* 262: 56–73
- Ginhoux F, Jung S (2014) Monocytes and macrophages: developmental pathways and tissue homeostasis. *Nat Rev Immunol* 14: 392–404
- Ginhoux F, Guillemins M (2016) Tissue-resident macrophage ontogeny and homeostasis. *Immunity* 44: 439–449
- Godwin JW, Pinto AR, Rosenthal NA (2013) Macrophages are required for adult salamander limb regeneration. *Proc Natl Acad Sci USA* 110: 9415–9420
- Gomez-Nicola D, Perry VH (2016) Analysis of microglial proliferation in Alzheimer's disease. *Methods Mol Biol* 1303: 185–193
- Gow DJ, Sauter KA, Pridans C, Moffat L, Sehgal A, Stutchfield BM, Raza S, Beard PM, Tsai YT, Bainbridge G, Boner PL, Fici G, Garcia-Tapia D, Martin RA, Oliphant T, Shelly JA, Tiwari R, Wilson TL, Smith LB, Mabbott NA et al (2014) Characterisation of a novel Fc conjugate of macrophage colony-stimulating factor. *Mol Ther* 22: 1580–1592
- Guarente L (2013) Calorie restriction and sirtuins revisited. *Genes Dev* 27: 2072–2085
- Guillemins M, De Kleer I, Henri S, Post S, Vanhoutte L, De Prijck S, Deswarte K, Malissen B, Hammad H, Lambrecht BN (2013) Alveolar macrophages develop from fetal monocytes that differentiate into long-lived cells in the first week of life via GM-CSF. *J Exp Med* 210: 1977–1992
- Haigis MC, Sinclair DA (2010) Mammalian sirtuins: biological insights and disease relevance. *Annu Rev Pathol* 5: 253–295
- Han MK, Song EK, Guo Y, Ou X, Mantel C, Broxmeyer HE (2008) SIRT1 regulates apoptosis and Nanog expression in mouse embryonic stem cells by controlling p53 subcellular localization. *Cell Stem Cell* 2: 241–251
- Harbour JW, Dean DC (2000) The Rb/E2F pathway: expanding roles and emerging paradigms. *Genes Dev* 14: 2393–2409
- Hashimoto T, Perlot T, Rehman A, Trichereau J, Ishiguro H, Paolino M, Sigl V, Hanada T, Hanada R, Lipinski S, Wild B, Camargo SM, Singer D, Richter A, Kuba K, Fukamizu A, Schreiber S, Clevers H, Verrey F, Rosenstiel P et al (2012) ACE2 links amino acid malnutrition to microbial ecology and intestinal inflammation. *Nature* 487: 477–481
- Hashimoto D, Chow A, Noizat C, Teo P, Beasley MB, Leboeuf M, Becker CD, See P, Price J, Lucas D, Greter M, Mortha A, Boyer SW, Forsberg EC, Tanaka M, van Rooijen N, Garcia-Sastre A, Stanley ER, Ginhoux F, Frenette PS et al (2013) Tissue-resident macrophages self-maintain locally throughout adult life with minimal contribution from circulating monocytes. *Immunity* 38: 792–804
- Haw R, Hermjakob H, D'Eustachio P, Stein L (2011) Reactome pathway analysis to enrich biological discovery in proteomics data sets. *Proteomics* 11: 3598–3613
- Hill R, Kalathur RK, Callejas S, Colaco L, Brandao R, Serelde B, Cebria A, Blanco-Aparicio C, Pastor J, Futschik M, Dopazo A, Link W (2014) A novel phosphatidylinositol 3-kinase (PI3K) inhibitor directs a potent FOXO-dependent, p53-independent cell cycle arrest phenotype characterized by the differential induction of a subset of FOXO-regulated genes. *Breast Cancer Res* 16: 482
- Hoekman MF, Jacobs FM, Smidt MP, Burbach JP (2006) Spatial and temporal expression of FoxO transcription factors in the developing and adult murine brain. *Gene Expr Patterns* 6: 134–140
- Hoffman B, Liebermann DA (2008) Apoptotic signaling by c-MYC. *Oncogene* 27: 6462–6472
- Houtkooper RH, Pirinen E, Auwerx J (2012) Sirtuins as regulators of metabolism and healthspan. *Nat Rev Mol Cell Biol* 13: 225–238

- Imai S, Armstrong CM, Kaerberlein M, Guarente L (2000) Transcriptional silencing and longevity protein Sir2 is an NAD-dependent histone deacetylase. *Nature* 403: 795–800
- Izarray RA, Hobbs B, Collin F, Beazer-Barclay YD, Antonellis KJ, Scherf U, Speed TP (2003) Exploration, normalization, and summaries of high density oligonucleotide array probe level data. *Biostatistics* 4: 249–264
- Jackson MD, Schmidt MT, Oppenheimer NJ, Denu JM (2003) Mechanism of nicotinamide inhibition and transglycosylation by Sir2 histone/protein deacetylases. *J Biol Chem* 278: 50985–50998
- Jenkins SJ, Ruckerl D, Thomas GD, Hewitson JP, Duncan S, Brombacher F, Maizels RM, Hume DA, Allen JE (2013) IL-4 directly signals tissue-resident macrophages to proliferate beyond homeostatic levels controlled by CSF-1. *J Exp Med* 210: 2477–2491
- Kaerberlein M, McVey M, Guarente L (1999) The SIR2/3/4 complex and SIR2 alone promote longevity in *Saccharomyces cerevisiae* by two different mechanisms. *Genes Dev* 13: 2570–2580
- Kenyon C (2005) The plasticity of aging: insights from long-lived mutants. *Cell* 120: 449–460
- Kitamura YI, Kitamura T, Kruse JP, Raum JC, Stein R, Gu W, Accili D (2005) FoxO1 protects against pancreatic beta cell failure through NeuroD and MafA induction. *Cell Metab* 2: 153–163
- Klotz LO, Sanchez-Ramos C, Prieto-Arroyo I, Urbanek P, Steinbrenner H, Monsalve M (2015) Redox regulation of FoxO transcription factors. *Redox Biol* 6: 51–72
- Lavin Y, Mortha A, Rahman A, Merad M (2015) Regulation of macrophage development and function in peripheral tissues. *Nat Rev Immunol* 15: 731–744
- Liu L, Rando TA (2011) Manifestations and mechanisms of stem cell aging. *J Cell Biol* 193: 257–266
- Mao B, Zhao G, Lv X, Chen HZ, Xue Z, Yang B, Liu DP, Liang CC (2011) Sirt1 deacetylates c-Myc and promotes c-Myc/Max association. *Int J Biochem Cell Biol* 43: 1573–1581
- Marshall GM, Liu PY, Gherardi S, Scarlett CJ, Bedalov A, Xu N, Iraci N, Valli E, Ling D, Thomas W, van Bekkum M, Sekyere E, Jankowski K, Trahair T, Mackenzie KL, Haber M, Norris MD, Biankin AV, Perini G, Liu T (2011) SIRT1 promotes N-Myc oncogenesis through a positive feedback loop involving the effects of MKP3 and ERK on N-Myc protein stability. *PLoS Genet* 7: e1002135
- Martins R, Lithgow GJ, Link W (2016) Long live FOXO: unraveling the role of FOXO proteins in aging and longevity. *Aging Cell* 15: 196–207
- McEvoy RC, Andersson J, Sandler S, Hellerstrom C (1984) Multiple low-dose streptozotocin-induced diabetes in the mouse. Evidence for stimulation of a cytotoxic cellular immune response against an insulin-producing beta cell line. *J Clin Invest* 74: 715–722
- Medema RH, Kops GJ, Bos JL, Burgering BM (2000) AFX-like Forkhead transcription factors mediate cell-cycle regulation by Ras and PKB through p27kip1. *Nature* 404: 782–787
- Menssen A, Hydring P, Kapelle K, Vervoorts J, Diebold J, Luscher B, Larsson LG, Hermeking H (2012) The c-MYC oncoprotein, the NAMPT enzyme, the SIRT1-inhibitor DBC1, and the SIRT1 deacetylase form a positive feedback loop. *Proc Natl Acad Sci USA* 109: E187–E196
- Merico D, Isserlin R, Stueker O, Emili A, Bader GD (2010) Enrichment map: a network-based method for gene-set enrichment visualization and interpretation. *PLoS ONE* 5: e13984
- Mildner A, Yona S, Jung S (2013) A close encounter of the third kind: monocyte-derived cells. *Adv Immunol* 120: 69–103
- Moffat J, Grueneberg DA, Yang X, Kim SY, Kloepper AM, Hinkle G, Piquini B, Eisenhaure TM, Luo B, Grenier JK, Carpenter AE, Foo SY, Stewart SA, Stockwell BR, Hacohen N, Hahn WC, Lander ES, Sabatini DM, Root DE (2006) A lentiviral RNAi library for human and mouse genes applied to an arrayed viral high-content screen. *Cell* 124: 1283–1298
- Motta MC, Divecha N, Lemieux M, Kamel C, Chen D, Gu W, Bultsma Y, McBurney M, Guarente L (2004) Mammalian SIRT1 represses forkhead transcription factors. *Cell* 116: 551–563
- Nakahata Y, Kaluzova M, Grimaldi B, Sahar S, Hirayama J, Chen D, Guarente LP, Sassone-Corsi P (2008) The NAD⁺-dependent deacetylase SIRT1 modulates CLOCK-mediated chromatin remodeling and circadian control. *Cell* 134: 329–340
- Niu B, Wu J, Mu H, Li B, Wu C, He X, Bai C, Li G, Hua J (2016) miR-204 regulates the proliferation of dairy goat spermatogonial stem cells via targeting to Sirt1. *Rejuvenation Res* 19: 120–130
- North BJ, Verdin E (2004) Sirtuins: Sir2-related NAD-dependent protein deacetylases. *Genome Biol* 5: 224
- Nowak K, Killmer K, Gessner C, Lutz W (2007) E2F-1 regulates expression of FOXO1 and FOXO3a. *Biochem Biophys Acta* 1769: 244–252
- Oh J, Lee YD, Wagers AJ (2014) Stem cell aging: mechanisms, regulators and therapeutic opportunities. *Nat Med* 20: 870–880
- Perdiguer EG, Geissmann F (2016) The development and maintenance of resident macrophages. *Nat Immunol* 17: 2–8
- Perry VH, Nicoll JA, Holmes C (2010) Microglia in neurodegenerative disease. *Nat Rev Neurol* 6: 193–201
- Petrie TA, Strand NS, Yang CT, Rabinowitz JS, Moon RT (2014) Macrophages modulate adult zebrafish tail fin regeneration. *Development* 141: 2581–2591
- Pietrocola F, Izzo V, Niso-Santano M, Vacchelli E, Galluzzi L, Maiuri MC, Kroemer G (2013) Regulation of autophagy by stress-responsive transcription factors. *Semin Cancer Biol* 23: 310–322
- Poulose N, Raju R (2015) Sirtuin regulation in aging and injury. *Biochem Biophys Acta* 1852: 2442–2455
- Prinz M, Priller J, Sisodia SS, Ransohoff RM (2011) Heterogeneity of CNS myeloid cells and their roles in neurodegeneration. *Nat Neurosci* 14: 1227–1235
- Prinz M, Priller J (2014) Microglia and brain macrophages in the molecular age: from origin to neuropsychiatric disease. *Nat Rev Neurosci* 15: 300–312
- Prinz M, Erny D, Hagemeyer N (2017) Ontogeny and homeostasis of CNS myeloid cells. *Nat Immunol* 18: 385–392
- Rathbone CR, Booth FW, Lees SJ (2009) Sirt1 increases skeletal muscle precursor cell proliferation. *Eur J Cell Biol* 88: 35–44
- Rimmele P, Bigarella CL, Liang R, Izac B, Dieguez-Gonzalez R, Barbet G, Donovan M, Brugnara C, Blander JM, Sinclair DA, Ghaffari S (2014) Aging-like phenotype and defective lineage specification in SIRT1-deleted hematopoietic stem and progenitor cells. *Stem Cell Reports* 3: 44–59
- Robbins CS, Hilgendorf I, Weber GF, Theurl I, Iwamoto Y, Figueiredo JL, Gorbato R, Sukhova GK, Gerhardt LM, Smyth D, Zavitz CC, Shikata EA, Parsons M, van Rooijen N, Lin HY, Husain M, Libby P, Nahrendorf M, Weissleder R, Swirski FK (2013) Local proliferation dominates lesional macrophage accumulation in atherosclerosis. *Nat Med* 19: 1166–1172
- Ruckerl D, Jenkins SJ, Laqtom NN, Gallagher IJ, Sutherland TE, Duncan S, Buck AH, Allen JE (2012) Induction of IL-4/alpha-dependent microRNAs identifies PI3K/Akt signaling as essential for IL-4-driven murine macrophage proliferation *in vivo*. *Blood* 120: 2307–2316
- Saldeen J, Tillmar L, Karlsson E, Welsh N (2003) Nicotinamide- and caspase-mediated inhibition of poly(ADP-ribose) polymerase are associated with p53-independent cell cycle (G2) arrest and apoptosis. *Mol Cell Biochem* 243: 113–122

- Satoh A, Brace CS, Rensing N, Cliften P, Wozniak DF, Herzog ED, Yamada KA, Imai S (2013) Sirt1 extends life span and delays aging in mice through the regulation of Nk2 homeobox 1 in the DMH and LH. *Cell Metab* 18: 416–430
- Saunders LR, Sharma AD, Tawney J, Nakagawa M, Okita K, Yamanaka S, Willenbring H, Verdin E (2010) miRNAs regulate SIRT1 expression during mouse embryonic stem cell differentiation and in adult mouse tissues. *Aging (Albany NY)* 2: 415–431
- Sauve AA, Schramm VL (2003) Sir2 regulation by nicotinamide results from switching between base exchange and deacetylation chemistry. *Biochemistry* 42: 9249–9256
- Schmidt M, Fernandez de Mattos S, van der Horst A, Klompmaier R, Kops GJ, Lam EW, Burgering BM, Medema RH (2002) Cell cycle inhibition by FoxO forkhead transcription factors involves downregulation of cyclin D. *Mol Cell Biol* 22: 7842–7852
- Schreiber E, Matthias P, Muller MM, Schaffner W (1989) Rapid detection of octamer binding proteins with 'mini-extracts', prepared from a small number of cells. *Nucleic Acids Res* 17: 6419
- Seoane J, Le HV, Shen L, Anderson SA, Massague J (2004) Integration of Smad and forkhead pathways in the control of neuroepithelial and glioblastoma cell proliferation. *Cell* 117: 211–223
- Sharma A, Gautam V, Costantini S, Paladino A, Colonna G (2012) Interatomic and pharmacological insights on human sirt-1. *Front Pharmacol* 3: 40
- Sherr CJ (1995) Mammalian G1 cyclins and cell cycle progression. *Proc Assoc Am Physicians* 107: 181–186
- Sherr CJ (1996) Cancer cell cycles. *Science* 274: 1672–1677
- Sherr CJ, Roberts JM (1999) CDK inhibitors: positive and negative regulators of G1-phase progression. *Genes Dev* 13: 1501–1512
- Shi C, Pamer EG (2011) Monocyte recruitment during infection and inflammation. *Nat Rev Immunol* 11: 762–774
- Sieweke MH, Allen JE (2013) Beyond stem cells: self-renewal of differentiated macrophages. *Science* 342: 1242974
- Sinclair DA, Guarente L (1997) Extrachromosomal rDNA circles—a cause of aging in yeast. *Cell* 91: 1033–1042
- Singh SK, Williams CA, Klarmann K, Burkett SS, Keller JR, Oberdoerffer P (2013) Sirt1 ablation promotes stress-induced loss of epigenetic and genomic hematopoietic stem and progenitor cell maintenance. *J Exp Med* 210: 987–1001
- Smyth GK (2004) Linear models and empirical bayes methods for assessing differential expression in microarray experiments. *Stat Appl Genet Mol Biol* 3: Article3
- Soucie EL, Weng Z, Geirsdottir L, Molawi K, Maurizio J, Fenouil R, Mossadegh-Keller N, Gimenez G, VanHille L, Beniazza M, Favret J, Berruyer C, Perrin P, Hacoen N, Andrau JC, Ferrier P, Dubreuil P, Sidow A, Sieweke MH (2016) Lineage-specific enhancers activate self-renewal genes in macrophages and embryonic stem cells. *Science* 351: aad5510
- Spector R (1987) Niacinamide transport through the blood-brain barrier. *Neurochem Res* 12: 27–31
- Spinelli L, Carpentier S, Montanana Sanchis F, Dalod M, Vu Manh TP (2015) BubbleGUM: automatic extraction of phenotype molecular signatures and comprehensive visualization of multiple Gene Set Enrichment Analyses. *BMC Genom* 16: 814
- Stanley ER (1985) The macrophage colony-stimulating factor, CSF-1. *Methods Enzymol* 116: 564–587
- Stevens C, La Thangue NB (2003) E2F and cell cycle control: a double-edged sword. *Arch Biochem Biophys* 412: 157–169
- Subramanian A, Tamayo P, Mootha VK, Mukherjee S, Ebert BL, Gillette MA, Paulovich A, Pomeroy SL, Golub TR, Lander ES, Mesirov JP (2005) Gene set enrichment analysis: a knowledge-based approach for interpreting genome-wide expression profiles. *Proc Natl Acad Sci USA* 102: 15545–15550
- Tissenbaum HA, Guarente L (2001) Increased dosage of a sir-2 gene extends lifespan in *Caenorhabditis elegans*. *Nature* 410: 227–230
- Tothova Z, Kollipara R, Huntly BJ, Lee BH, Castrillon DH, Cullen DE, McDowell EP, Lazo-Kallanian S, Williams IR, Sears C, Armstrong SA, Passegue E, DePinho RA, Gilliland DG (2007) FoxOs are critical mediators of hematopoietic stem cell resistance to physiologic oxidative stress. *Cell* 128: 325–339
- Tsuchiya K, Westerterp M, Murphy AJ, Subramanian V, Ferrante AW Jr, Tall AR, Accili D (2013) Expanded granulocyte/monocyte compartment in myeloid-specific triple FoxO knockout increases oxidative stress and accelerates atherosclerosis in mice. *Circ Res* 112: 992–1003
- Venter G, Oerlemans FT, Willemse M, Wijers M, Fransen JA, Wieringa B (2014) NAMPT-mediated salvage synthesis of NAD⁺ controls morphofunctional changes of macrophages. *PLoS ONE* 9: e97378
- Vogt PK, Jiang H, Aoki M (2005) Triple layer control: phosphorylation, acetylation and ubiquitination of FOXO proteins. *Cell Cycle* 4: 908–913
- Waisman A, Ginhoux F, Greter M, Bruttger J (2015) Homeostasis of microglia in the adult brain: review of novel microglia depletion systems. *Trends Immunol* 36: 625–636
- Webb AE, Brunet A (2014) FOXO transcription factors: key regulators of cellular quality control. *Trends Biochem Sci* 39: 159–169
- Wong S, Weber JD (2007) Deacetylation of the retinoblastoma tumour suppressor protein by SIRT1. *Biochem J* 407: 451–460
- Wong DJ, Liu H, Ridky TW, Cassarino D, Segal E, Chang HY (2008) Module map of stem cell genes guides creation of epithelial cancer stem cells. *Cell Stem Cell* 2: 333–344
- Wynn TA, Chawla A, Pollard JW (2013) Macrophage biology in development, homeostasis and disease. *Nature* 496: 445–455
- Yuan J, Minter-Dykhouse K, Lou Z (2009) A c-Myc-SIRT1 feedback loop regulates cell growth and transformation. *J Cell Biol* 185: 203–211
- Yuan HF, Zhai C, Yan XL, Zhao DD, Wang JX, Zeng Q, Chen L, Nan X, He LJ, Li ST, Yue W, Pei XT (2012) SIRT1 is required for long-term growth of human mesenchymal stem cells. *J Mol Med (Berl)* 90: 389–400
- Zhang X, Tang N, Hadden TJ, Rishi AK (2011) Akt, FoxO and regulation of apoptosis. *Biochem Biophys Acta* 1813: 1978–1986
- Zhang Q, Zeng SX, Zhang Y, Zhang Y, Ding D, Ye Q, Meroueh SO, Lu H (2012) A small molecule Inauhizin inhibits SIRT1 activity and suppresses tumour growth through activation of p53. *EMBO Mol Med* 4: 298–312
- Zhang H, Ryu D, Wu Y, Gariani K, Wang X, Luan P, D'Amico D, Ropelle ER, Lutolf MP, Aebersold R, Schoonjans K, Menzies KJ, Auwerx J (2016a) NAD (+) repletion improves mitochondrial and stem cell function and enhances life span in mice. *Science* 352: 1436–1443
- Zhang QB, Cao W, Liu YR, Cui SM, Yan YY (2016b) Effects of Sirtuin 1 on the proliferation and osteoblastic differentiation of periodontal ligament stem cells and stem cells from apical papilla. *Genet Mol Res* 15: gmr5234